Final Technical Report
NAG5-3209

Date:	December 6, 1999
PI:	Dr. Mark Dickinson, Space Science Telescope Institute
NASA Grant No:	NAG5-3209
Title:	*The Most Distant X-Ray Clusters*
STScI Project No:	J0467
Performance Pd:	05/01/96 - 09/30/99
STScI Grant Administrator:	Larisa Dolhancryk 3700 San Martin Drive, Baltimore, MD 21218 Phone: 410.338.4364 Email: larisad@stsci.edu

In this program we have used ROSAT to observe X-ray emission around several high redshift radio galaxies in a search for extended, hot plasma which may indicate the presence of a rich galaxy cluster. When this program was begun, massive, X-ray emitting galaxy clusters were known to exist out to to $z=0.8$, but no more distant examples had been identified. However, we had identified several apparently rich clusters around 3CR radio galaxies at $z > 0.8$, and hoped to use ROSAT to confirm the nature of these structures as massive, virialized clusters.

Over the course of several previous cycles of ROSAT observations, we had used the PSPC to detect X-ray emission from radio galaxies, but were unable to distinguish between emission from the active nucleus and from extended cluster gas. In order to do so, in this program we obtained very deep reobservations with the ROSAT HRI to determine whether or not the X-ray emission was spatially extended. In general, given the limited sensitivity of the HRI to very faint extended emission, we did not expect to robustly detect the emission if it was extended. Rather, the HRI observations were used as a sort of spatial high pass filter on the PSPC data. Knowing the X-ray flux from the source in advance from the PSPC, we could predict the expected count rate with the HRI, and set our exposures so that we would easily see the emission if it arose from a nuclear (AGN) point source. If no such point sources were detected, it would be likely that the X-rays arose from a spatially extended plasma, i.e. intracluster gas.

We observed four radio galaxies altogether, with $0.99 < z < 1.78$. Not all had previous/ancillary evidence for the presence of clusters, e.g. from optical or infrared data, but several (e.g., 3C324) did. In all cases, we measured X-ray fluxes with the HRI which were consistent with the previous PSPC data. In two cases, 3C324 and 3C294, we found that the X-ray emission was definitely extended. 3C324 was an important test case, because we have outstanding spectroscopic data on this field from Keck which confirms the reality of the apparent galaxy cluster. 3C294 has very little supporting optical data due to the presence of a very bright star in the field. The extended X-ray detection here, however, is extremely interesting: 3C294 has the highest redshift in our sample, $z=1.78$.

The extended X-rays therefore make this likely to be the most distant X-ray cluster known. We have proposed to HST and Chandra to obtain supporting optical/UV and X-ray imaging, and will be studying the field in the infrared with an Adaptive Optics system at CFHT next spring.

For 3C280 the results were somewhat ambiguous although consistent with the presence of both resolved and unresolved components, and for a fourth galaxy, 3C194, the emission appears to be unresolved. The final ROSAT observations for this project were never completed due to the demise of the satellite and the cessation of the ROSAT observing program.

The detection of extended X-ray emission from 3C324 and 3C294, both having X-ray luminosities approaching 10^45 erg/s, is important because (1) it establishes that luminous X-ray clusters do exist at $z > 1$, and probably out to nearly $z=2$, (2) it verifies that high redshift radio galaxies often inhabit dense, virialized clusters, (3) it establishes that the cluster emission around these sources have central surface brightnesses that are substantially higher than those of most "normal" clusters nearby, possibly due to the presence of strong central cooling flows. Our models for this X-ray emission show that it is indeed likely that the central cooling time is shorter than the Hubble time at those redshifts, and therefore that cooling flows are likely.

We have written up our results and submitted them as a paper to the Astrophysical Journal. This paper has been refereed and requires some significant revisions to accommodate the referees' comments. We are in the process of doing this, adding some additional analysis as well. We will resubmit the paper early in 2000, and hopefully will meet with the referee's approval. We are including three copies of the submitted paper here, although it has not yet been accepted for publication.

Submitted to The Astrophysical Journal.

Extended X–ray Emission from Galaxy Clusters at $z > 1$

Mark Dickinson[1]
The Johns Hopkins University, Department of Physics and Astronomy, Baltimore MD 21218

Richard F. Mushotzky
Laboratory for High Energy Astrophysics, NASA/Goddard Space Flight Center, Code 662, Greenbelt MD 20771

Hyron Spinrad
Department of Astronomy, University of California, Berkeley CA 94720

Patrick J. McCarthy
Observatories of the Carnegie Institute of Washington, 813 Santa Barbara St., Pasadena CA 91101

and

Wil van Breugel
Institute for Geophysics and Planetary Physics, Lawrence Livermore National Laboratories, P.O. Box 808, Livermore CA 94550

ABSTRACT

We present ROSAT observations aimed at detecting and resolving X–ray emission from powerful 3CR radio galaxies at $z \gtrsim 1$. Data from the High Resolution Imager (HRI) is used to determine the spatial extent of X–ray emission previously detected by the Position Sensitive Proportional Counter (PSPC), and to set limits on point source contribution from the active nuclei of the radio galaxies. Out of five sources, one is nearly point–like and may be dominated by AGN emission. Two are somewhat ambiguous but probably include resolved emission, and two are undoubtedly extended over spatial scales of several hundred kpc. The manifestly extended sources are 3C 324, which is

[1]Allan C. Davis Fellow, also with the Space Telescope Science Institute

known to inhabit a rich galaxy cluster at $z = 1.206$, and 3C 294 at $z = 1.786$. The extended X–ray emission most likely arises from hot gas in a deep cluster potential well. 3C 294 is the most distant object for which such extended X–ray emission has been detected is therefore likely to be one of the most distant galaxy clusters known. The bolometric luminosities of the extended cluster emission from 3C 294 and 3C 324 are approximately 9×10^{44} erg s^{-1}, comparable to rich clusters at low redshift such as Coma as well as clusters around similarly powerful nearby radio galaxies such as Cygnus A and 3C 295. The X–ray emission from these $z > 1$ clusters is more compact and has higher central surface brightness than is the case for clusters like Coma. Without such high surface brightness it would be difficult to detect such clusters would be detectable in ROSAT data. Nor are the PSPC images alone (without additional information from the HRI data) adequate to demonstrate spatial extent for most of the objects. These facts highlight the difficulty of identifying X–ray clusters at $z > 1$ in "blank field" ROSAT surveys, i.e. without the benefit of an *a priori* target such as a radio source. We consider the properties of the clusters in as much detail as the limited X–ray data allow, and compare the lower limits on their space density to some simple theoretical predictions. Although the existing sample does not yet provide strong bounds on cluster evolution or cosmological parameters, the resulting limits are already sufficient that a future survey capable of detecting 10× more clusters at similar redshifts could prove quite constraining. Similarly, a reliable mass measurement for even a single cluster at $z \sim 2$ could provide tight limits on the cosmological model.

Subject headings: galaxies: clusters: general — galaxies: active — cosmology: observations — large–scale structure of universe — X–rays: galaxies

1. Introduction

Distant clusters of galaxies have long served as laboratories for studying both galaxy evolution and cosmic structure formation. Some of the first direct evidence for galaxy evolution was found in high redshift clusters when Butcher & Oemler (1978) noted an increasing abundance of blue, star forming galaxies at higher redshifts. More recently, studies of the early type (E/S0) galaxy population in high redshift clusters have provided detailed information about the evolution of these old stellar systems out to $z \approx 1$ (e.g. Aragón–Salamanca *et al.* 1993; Ellis *et al.* 1997; van Dokkum & Franx 1996; Dickinson 1997*c*; Stanford *et al.* 1998). As the most massive bound gravitational systems in the

universe, galaxy clusters also provide important information about the nature and evolution of cosmological mass fluctuations. For this purpose, X–ray and gravitational lensing studies have proven to be particularly important, as they manifest the effects of the gravitational potential. For all of these reasons, observers have sought to find ever more distant examples of rich galaxy clusters in order to push these investigations back to earlier cosmic look–back times.

Optical and X–ray surveys for high redshift clusters have provided extensive samples out to $z \approx 1$ (e.g. Gunn, Hoessel & Oke 1984; Couch *et al.* 1991; Gioia *et al.* 1990, 1994; Postman *et al.* 1996) but little information beyond that redshift. During the ROSAT era, systematic wide–field surveys of X–ray sources have identified many new clusters at $0.4 \lesssim z \lesssim 0.8$ (e.g. Rosati *et al.* 1995, 1998; Castander *et al.* 1995; Scharf *et al.* 1997; Collins *et al.* 1997; Henry *et al.* 1997; Vikhlinin *et al.* 1998), but none (so far) at higher redshifts. However, this may not imply any genuine deficit of clusters at larger redshift. Current evidence from optical and X–ray selected samples suggests little change in the space density of clusters with "typical" richnesses or luminosities out to $z \approx 0.8$ (e.g. Postman *et al.* 1996; Rosati *et al.* 1998), so there is little reason to expect a sudden decline just beyond that redshift. Instead, the lack of $z > 0.9$ clusters in current surveys may simply reflect the difficulty of finding such systems with existing X–ray data and following them up with imaging and spectroscopy from 4m–class telescopes. Even very luminous X–ray clusters at $z > 1$ would be faint sources near the ROSAT detection limits, and optical follow–up of cluster galaxies and spectroscopic confirmation of their redshifts is extremely difficult at such large redshifts. The few convincing examples of galaxy clusters at $z > 1$ have mostly been found in targeted searches, often by examining the environments of powerful radio–loud AGN (cf. Dickinson 1997*a*, *b* for reviews). Another example found in a targeted search is an extended X–ray source, seemingly an "optically dark" galaxy cluster at $z = 1.01$ along the sightline to the distant gravitational lens system MG 2016+112 (Hattori *et al.* 1997). Recently, Stanford *et al.* (1997) identified a cluster of galaxies at $z = 1.27$ in a near–infrared field galaxy survey. *Post facto* inspection of archival ROSAT images revealed a corresponding X–ray source, making this the first and (to date) only X–ray emitting cluster at $z > 1$ identified from an untargeted survey.

The targeted searches for high redshift clusters have been inspired by the evidence that powerful radio galaxies and quasars at $z < 1$ are often situated in cluster environments (cf. Yee & Green 1984; Yates, Miller & Peacock 1989; Hill & Lilly 1991; Allington–Smith *et al.* 1993, Dickinson 1994). Observations of low redshift radio galaxies have demonstrated that X–ray emission may be comprised of several components, including thermal emission from the cluster environment and non–thermal emission from the active galactic nucleus (AGN). This complicates the interpretation of X–ray measurements for distant radio

galaxies unless data with adequate angular resolution and signal–to–noise can be obtained to distinguish between the various possible sources of emission.

Here we present results from a small X–ray survey of powerful radio galaxies at $z \gtrsim 1$. Observations with low and high angular resolution instruments are used together in order to assess the spatial extent of X–ray emission around five powerful FR II radio galaxies in order to distinguish between AGN and cluster sources. We find that at least two, and perhaps all of the radio galaxies are surrounded by highly luminous atmospheres of X–ray emitting gas whose properties are similar to those of nearby rich clusters of galaxies. By analogy, then, we infer that these radio galaxies inhabit massive clusters at $1 < z < 2$. In one case there is substantial supporting evidence for the presence of a cluster from optical and near–infrared observations of the associated galaxies. In §2 we describe the ROSAT observations and basic analysis. §3 provides information on each of the individual radio galaxy fields. In §4 we compare the X–ray properties of these distant clusters to their more local counterparts, and briefly consider the implications of the existence of such clusters for theories of structure formation and for cosmological models. Conclusions and discussion are presented in §5. For the purposes of computing sizes, luminosities and masses from the observed data we have assumed an Einstein–de Sitter cosmology ($\Omega_M = 1$, $\Lambda = 0$) with $H_0 = 50$ km s^{-1} Mpc^{-1} throughout this paper. Occasionally we will use the notation h or h_{50} to indicate H_0 in units of 100 or 50 km s^{-1} Mpc^{-1}.

2. Observations and X–ray Image Analysis

During the first four years of ROSAT operations we carried out a program of X–ray imaging of powerful radio galaxies at $z > 1$ using the Position Sensitive Proportional Counter (PSPC). Altogether we observed seven radio galaxies with exposure times which ranged from 6 to 35 ksec; two other targets received exposures < 4 ksec due to telescope failures. All but one of the radio galaxies was drawn from the 3CR catalog. At the time the observations were proposed virtually nothing was known about the environments of radio galaxies at these redshifts, and our targets were not selected with any *a priori* predisposition to clusters. Instead, the targets were chosen partly on the basis of how much supporting ground–based data was in hand at the time, and partly by the strength of their [OII] 3727Å or Lyman α emission lines. In addition, three other $z \gtrsim 1$ 3CR radio galaxies were observed by other investigators: 3C 280 (Worrall *et al.* 1994), 3C 356 and 3C 368 (Crawford & Fabian 1993, 1995). Archival PSPC data on distant radio galaxies has been compiled and analyzed in the literature by Crawford & Fabian (1996*b*).

Nearly all of the radio galaxy targets were detected as X–ray sources with the PSPC,

mostly at the ~ 5 to 8σ level. A few objects (e.g. 3C 210 and 3C 256) were only marginally detected ($\lesssim 3\sigma$); only the positional coincidence of these weak sources with *a priori* radio coordinates makes their reality plausible. Here we restrict our attention to five radio galaxies with the highest and most secure X–ray fluxes for which follow–up observations at higher angular resolution were possible.

For most of the radio galaxies, the poor signal–to–noise ratio of the X–ray detections and the low angular resolution of the PSPC (FWHM $\approx 25''$) preclude secure determination of whether or not the X–ray emission is spatially extended. Similarly, meaningful spectral analysis is generally not feasible. Thus in most cases the question of whether or not the X–rays arise from the radio galaxy AGN or in a surrounding cluster environment remains unanswered by the PSPC data alone. In order to address this matter we used the High Resolution Imager (HRI) to re–observe four of the brightest sources which had previously been detected with the PSPC. Crawford & Fabian (1996*a*) have described their HRI observations a fifth radio galaxy, 3C 356; we include our own analysis of their data here for purposes of uniformity.

At high redshift the effect of cosmological surface brightness dimming is severe, making it difficult to observe extended emission from galaxy clusters. Moreover, the ROSAT HRI is less sensitive than the PSPC and has a significantly higher background count rate per unit solid angle, making it rather insensitive to diffuse, low surface–brightness emission. However, the angular resolution of the HRI (FWHM $\approx 4''$) makes it an outstanding point source detector. The experiment we carried out with the HRI is simple: given the known X–ray flux of our targets as measured by the PSPC, we exposed with the HRI long enough to obtain a firm ($\gtrsim 5\sigma$) detection of the X–ray emission *if* it arose primarily from an unresolved nuclear point source, i.e. an AGN. If, instead, the X–ray emission is extended, it should be largely "resolved out" by the HRI, detected at best as a low S/N diffuse signal within some large aperture. Thus we do not expect to produce beautiful X–ray maps of clusters at $z > 1$ – a source with X–ray luminosity similar to that of the Coma cluster should barely be detected by the ROSAT HRI at $z > 1$, even with 40 to 100 ksec of exposure time, unless it were actually dominated by an unresolved point source. The HRI observations serve, in effect, as a spatial high–pass filter on the PSPC detections.

Table 1 summarizes the X–ray properties of the five radio galaxies studied here. In all cases, analysis was performed on data processed using Revision 2 of the Standard Analysis Software System (SASS) pipeline. Two dimensional image processing was done using IRAF and the PROS X–ray analysis software. The HRI observations of 3C 280 were obtained in two separate exposure sequences with integration times of 53.3 and 9.7 ksec. These were shifted into registration with one another using the positions of several well–detected point

sources in the image and the photon event (QPOE) files were combined to produce a single data set which was used for the analysis presented here. Then, for each field the HRI and PSPC images were registered using the positions of several serendipitous point sources.

Figure 1 (Plate X) shows portions of the PSPC and HRI images for four of the five radio galaxies. The images for 3C 356 have previously been presented by Crawford & Fabian (1993, 1996*a*). To graphically illustrate the experiment being carried out, a false point source has been added to each HRI image to show how the X–ray source would appear *if* all of the flux arose from an AGN nucleus. The artificial sources were generated using the HRI point response function (PRF) taken from David *et al.* (1997). The flux in the false point source is scaled to the HRI count rate predicted on the basis of the flux measured from the PSPC image (see discussion below and Table 1). Poisson noise was added before the point source was added into the real HRI image. The actual PRF of a given ROSAT HRI observation may be different, generally broader, than the David *et al.* model due to aspect solution errors. For this reason, the false point sources should only be used for the purpose of visual comparison to the radio galaxy source. Actual flux profile comparisons (figures 4–8) have been made using other real point sources present in the same images rather than the synthetic PRFs.

By inspecting figure 1 it is easy to see that some of the radio galaxies are not recovered as point sources (e.g. 3C 324 and 3C 294), while others are compact and may be consistent with the point source model (e.g. 3C 194). We consider each object in detail below. Also shown in figure 1 are smoothed versions of the HRI images, which generally reveal a faint source present at the radio galaxy position, albeit at low signal–to–noise. This is as expected – the HRI observations were intended to robustly detect the X–ray source *only* if a substantial fraction of the PSPC flux arose in an unresolved component. If the source is significantly extended beyond the scale of the point response function then we would *not* expect to see a strong detection in the HRI images. Indeed 3C 324 is nearly invisible in the unsmoothed HRI data, having been fully resolved out.

Source centroid positions were measured directly from the ROSAT images whenever possible and used as fixed centers for aperture flux measurements. The HRI images of all fields except 3C 324 have faint sources visible near the positions of the radio galaxies which were used as the center positions – in these cases the HRI positions are in excellent agreement ($< 4''$) with the radio, optical and infrared positions of the radio galaxies. For 3C 324 the X–ray emission is too diffuse for an accurate centroid to be computed from the HRI image. In this case the position of the X–ray source measured from the PSPC image has been used has been used to define the center of the HRI photometric aperture.

Photon counts in the PSPC data were measured in PI channels 41—240, spanning

energies from 0.4 to 2.4 keV, where the instrumental background is minimized. All measurements were made through circular apertures, and the values reported in Table 1 are those determined within a radius of 40″. This corresponds to a physical radius $\approx$ 340 kpc at $1 < z < 2$ for the cosmology assumed here and encompasses most of the flux from an unresolved source in PSPC data, although it may underestimate the total flux for extended sources. The background was measured from a larger annulus (40″ to 80″ radius) which was inspected to ensure that there was no flux contributions from other nearby sources. Measurement uncertainties reported in Table 1 are Poisson errors for the object plus background. Conversion to flux units was made assuming a Raymond & Smith (1977) thermal plasma with $kT = 4$ keV and 0.3 $\times$ cosmic abundance, emitted at the radio galaxy redshift, and with foreground absorption appropriate for the galactic N_H value taken from Stark *et al.* (1992). The exact flux conversion is only weakly dependent on the assumed spectral model – varying the temperatures or abundances within plausible ranges generally results in flux differences that are smaller than the statistical uncertainty of the X–ray measurements. Luminosities were computed for the rest–frame 1–5 keV band, appropriate for the redshifted energy range sampled by the PSPC data and thus requiring only minimal k–corrections to the X–ray fluxes. Again, these corrections are nearly independent of the assumed spectral model. All conversions between instrumental counts, fluxes, and luminosities used in this paper were calculated using XSPEC (v10.0) from the XANADU software package (Arnaud 1996).

Also listed in Table 1 are the X–ray counts predicted for and measured from the HRI observations. The predicted counts were computed for the total HRI band (0.1–2.4 keV) using the observed PSPC fluxes, the model thermal spectrum, and the energy response matrix of the HRI. The uncertainties given for this quantity are just those of the PSPC measurement propagated through the conversion. These predicted HRI fluxes were used to produce the false point sources added into the images for figure 1, as described above.

The large–aperture HRI flux measurements in Table 1 show that in most cases the X–ray source is weakly detected as a positive signal in the HRI data, consistent with the impression given by the smoothed HRI images shown in figure 1. Figure 2 compares the predicted and measured HRI counts for the five radio galaxies. In all cases there is agreement within the errors. The positive HRI detections, while individually unimpressive, are important; any single X–ray source, if arising from an AGN, might have faded during the interval between the PSPC and HRI observations due to intrinsic source variability. It is quite unlikely, however, that the same would be true for all five radio galaxies which we have observed. The fact that the X–ray fluxes do not vary between the PSPC and HRI observations is a necessary (but not sufficient) condition that the emission is due to extended thermal plasma and not an active nucleus.

One indication of spatial extent is given by a comparison of fluxes measured within small and large apertures, which provides a measure of the image concentration or peakedness. The PRF of the HRI is such that approximately 75% of the flux is enclosed within a 6″ radius aperture. Spatially extended sources will have a smaller encircled energy fraction within this radius. Figure 3 plots ratios of HRI fluxes in 6″ and 40″ radius apertures for the five radio galaxy sources and for serendipitous point sources in each field. 3C 194 and 3C 280 appear to be marginally extended in this test, but only at slightly more than 1σ confidence. The weak HRI source associated with 3C 356 is also compact – we discuss this in greater detail in §3.5 below. 3C 294 and 3C 324, however, have only 44% and 18% of their flux encircled within 6″ apertures, confirming their spatial extent.

3. Notes on individual sources:

Here we discuss each of the five radio galaxy sources individually. The accompanying figures (4–8) show azimuthally averaged surface brightness profiles and cumulative curves of growth for the X–ray emission from each radio galaxy in the PSPC and HRI images. In each case these are compared to the profiles of one or more serendipitous, compact (presumably point) sources in the same images. These point sources have been multiplicatively rescaled for these figures so that their aperture fluxes match those of the radio sources, thus allowing one to visually assess the spatial extent of the radio galaxy X–ray emission by comparison.

3.1. 3C 194 ($z = 1.184$):

This radio galaxy was first correctly identified by Djorgovski *et al.* (1988), but was published with an incorrect redshift. The actual redshift is 1.184 (Strom *et al.* 1990). Wide–field infrared and optical imaging reveals no compelling evidence for a local overdensity of galaxies which might correspond to a rich galaxy cluster (Dickinson & Eisenhardt, in preparation). Taylor, Inaoue & Tabara (1992) found that the 3C 194 radio source exhibits extremely large Faraday rotation measures (RMs), exceeding 1000 radians m^{-2}, with strong spatial variations over the radio hotspots. At lower redshifts, such strong RMs are invariably associated with radio sources in cooling–flow environments (e.g. Taylor, Barton & Ge 1994) – both Cygnus A and 3C 295, two of the only $z < 1$ analogs to the powerful 3CR sources studied here, are good examples. Talyor *et al.* therefore speculate that 3C 194 should be situated in a similar environment.

This is the most luminous of the five X–ray sources observed here, and is well detected

in the HRI images. Inspecting the radial profile of the X–ray source as seen in the PSPC and HRI (figure 4) and the image itself (figure 1), it is clear that most of the X–ray emission arises from a very compact source. The flux profile appears to be marginally broader than that of a point source in the field (figures 3 and 4), but is probably consistent with being unresolved. 3C 194 is thus a good case for an object whose X–ray emission may be dominated by the radio galaxy AGN. Of the five galaxies observed here, 3C 194 also has the strongest flat spectrum radio core (5.0 mJy at 5 GHz – Strom *et al.* 1990). For nearby radio galaxies, Feigelson & Berg (1983) and Fabbiano *et al.* (1984) found a good correlation between the 5 GHz radio core luminosity and X–ray luminosity. The logarithm of the ratio of X–ray to radio flux densities (at 2 keV and 5 GHz rest frame energy/frequency, respectively) for 3C 194 is approximately -5.7, which is also roughly the median value found for nearby FR II radio galaxies by Fabbiano *et al.* (1984). Although the photon statistics of the PSPC data are poor, Crawford & Fabian (1996*b*) have argued that a power law with soft energy absorption greatly in excess of the galactic foreground value provides an better fit to the X–ray photon energy distribution for 3C 194 than does a thermal plasma model. While better X–ray spectral data are required to confirm this result, it would be consistent with an AGN origin for the X–ray emission from 3C 194.

At the same time, the high Faraday RM found by Taylor *et al.* (1994) would suggest the presence of a dense cooling flow environment. In this case, we would have to interpret the compact X–ray emission as arising from very spatially concentrated ($\lesssim$ 50 kpc radius) cooling gas. The 3C 194 FR II radio source has a size of 15″ and is thus entirely contained within the X–ray emission region seen in the HRI image. If the marginal spatial extent implied by the HRI surface brightness profile and the flux ratio test were significant, then a cooling flow origin of at least part of the X–ray emission would still be plausible. The X–ray luminosity of 3C 194 would be wholly dominated by this cooling gas. Cooling flow luminosity is related to the mass deposition rate $\dot{M}$ by $L_{\rm cool} \approx 5\dot{M}kT/2\mu m_p$, where T is the initial gas temperature and μ and m_p are the mean mass per particle and proton mass, respectively (Stewart *et al.* 1984). The visibly detected HRI flux is mostly enclosed within an 12″ radius, where we find $25.8^{+7.4}_{-6.4}$ counts, corresponding to 63% of the total PSPC flux. If we assign this fraction of the X–ray luminosity (2.5×10^{44} erg s^{-1}, 1–5 keV) to a cooling flow region, this would correspond to an inflow rate $\dot{M} \approx 170(kT/4\ {\rm keV})^{-1} M_\odot$/year, similar to that observed for Cygnus A (Arnaud *et al.* 1987) and 3C 295 (Henry & Henriksen 1986).

Unfortunately, even our robust HRI detection of 3C 194 is therefore insufficient to firmly establish the origin of the X–ray emission from this system. Its spatial extent is consistent both with point–like and slightly extended distributions. AGN or compact cooling flow emission both may be viable sources. The former interpretation is credible because of the expected correlation between radio core luminosity and nuclear X–ray

emission, while the latter is supported by the anomalously large rotation measures observed for the radio source. Only X–ray observations with higher S/N and better spatial or spectral resolution can settle the issue.

3.2. 3C 280 ($z = 0.998$):

The PSPC observations of 3C 280 used here were obtained by Worrall *et al.* (1994), and are unusually deep (48 ksec) compared to the PSPC data on our other radio galaxy targets. Worrall *et al.* noted that the X–ray source appears to be spatially extended in the PSPC image. Those authors decomposed the source into extended and unresolved components and compared the X–ray to 5 GHz flux ratio to that of core–dominated radio loud quasars.

The HRI observation does indeed show a compact component, consistent with being a point source, which carries a substantial fraction of the total luminosity. Using the nominal coordinate solution for the HRI image, the apparent point source is situated at $\alpha = 12^h56^m57\overset{s}{.}74$, $\delta = 47°20'23\overset{''}{.}8$ (J2000), which is $< 4''$ away from the infrared and optical position of the radio galaxy itself as determined from HST and ground–based imaging (Best *et al.* 1997). This is well within the typical absolute uncertainties of astrometry from ROSAT HRI data ($6\overset{''}{.}4$ r.m.s. according to information supplied by the ROSAT Guest Observer Facility). We therefore consider it likely that the HRI point source is directly associated with the radio galaxy and quite probably with its active nucleus.

Whether there is in fact an additional extended component is less clear. Inspecting the images and the radial profile (figure 5), the source actually appears to be *more* extended in the PSPC than in the HRI. Indeed it is the only one of the sources presented here which appears visibly extended compared to the PSPC point response profile. The measurement of spatial extent in the PSPC data by Worrall *et al.* (1994) therefore seems to be well justified, whereas it is difficult to say the same from the HRI images alone. There does seem to be extra flux in the HRI image beyond the point source radius, but with low significance. The total flux recovered in the HRI data within a $40''$ radius aperture is 63% larger than the predicted value (Table 1), although the numbers are formally consistent within the errors. This is the largest discrepancy between predicted and measured counts seen among the five radio galaxies studied here. Given that the X–ray emission appears extended in the PSPC, with lower surface brightness than is typical for some the other sources considered here, it is not surprising that it should be difficult to detect in the HRI image; as already noted, the HRI is not sensitive to low surface brightness, extended emission. Perhaps more significantly, the HRI point source component alone has $27.6^{+7.6}_{-6.5}$ counts within an $8''$ radius aperture, nearly the entirety of the 29 counts predicted from the *seemingly extended* PSPC

flux. This apparent contradiction suggests that the luminosity of the nuclear point source increased from 1991 to 1996, the interval between the PSPC and HRI observations. For the moment, we consider the interpretation of the X–ray emission from 3C 280 to be somewhat ambiguous, although the presence of a compact, point–like source coincident with the radio galaxy is clear. The ROSAT data, taken together, is consistent with the presence of an extended, relatively low surface brightness cluster component plus a temporally variable nuclear point source.

3.3. 3C 294 ($z = 1.786$):

3C 294 was the subject of extensive investigation by McCarthy *et al.* (1990) who presented radio maps, optical spectroscopy, narrow band and infrared imaging. The galaxy has powerful ultraviolet line emission extended for $\sim$ 100 kpc along the radio source axis. The ionized gas exhibits a complex velocity structure with line widths and velocity gradients $\gtrsim 1000 - -2000$ km s^{-1}. Imaging of this field is severely hampered by the presence of a $V = 12$ K subgiant star which is located only 12″ away from the radio galaxy. There is therefore no information available about the galaxy environment of 3C 294, although in the future the bright star offers an excellent opportunity for the application of adaptive optics.

The ROSAT HRI source is clearly extended compared to both the real and simulated point sources (figures 1, 3 and 6). It is visibly detected in the HRI image, however, and thus (by the nature of our experiment) must be fairly compact. The simulated HRI point source in figure 1 and the rescaled profiles of real point sources in the field (figure 6) exhibit more compact flux distributions and much larger peak surface brightness for the same total flux. The spatial extent of the X–ray source confirms that it is not associated with the bright foreground star, and the positional agreement of the HRI flux centroid with 3C 294 itself is excellent. Assuming that the X–rays arises from a cluster environment, 3C 294 is the most distant cluster from which unambiguously extended X–ray emission has been detected.

3.4. 3C 324 ($z = 1.206$):

3C 324 has been the subject of extensive study from the ground and with HST (see Dickinson 1995*a*, *b*, 1997*a*, *b*, *c*). The radio galaxy is situated in a moderately rich cluster of galaxies, many of which have very red optical–infrared colors and the morphologies of mature elliptical galaxies. Spectroscopy from the Keck Observatory has confirmed the association of many of these galaxies with the radio source at $z = 1.21$, although a

foreground structure is also present at $z = 1.15$ (see Dickinson 1996*b*). Optical and infrared spectroscopic and imaging data on 3C 324 will be presented in detail in a future paper.

The X–ray emission from 3C 324 is extended – the HRI image resolves out the flux entirely (figure 1), with no evidence for a point source component. The PSPC flux is recovered, however, when a large aperture is used for the HRI measurement, as shown in figures 2 and 7. The curve of growth for the HRI source continues to rise out to a radius of $\sim 40''$, corresponding to a physical diameter of $\gtrsim 700$ kpc. This is substantially larger than the size of the FR II radio source ($11''$), thus ruling out any possibility that the inverse Compton process could be producing the X–ray emission. Faraday rotation and depolarization in the 3C 324 radio source have been studied by Pedelty *et al.* (1989) and Best *et al.* (1998*b*). The latter authors find modest RMs (100–200 radian m^{-2} in the rest frame) when averaging over the whole source, but with strong local variations of $\sim$ 1000 radian m^{-2} in the regions of strongest depolarization. This is similar to but less extreme than the situation found by Taylor *et al.* (1992) for 3C 194. The RMs are consistent with a Faraday screen produced by the intra–cluster medium external to the radio lobes. The smaller values would suggest a more modest cooling rate than is seen for anomalously high RM sources like 3C 295 (Taylor *et al.* 1994), consistent with the absence of any very centrally concentrated, high surface brightness X–ray component to 3C 324.

Smail & Dickinson (1995) used deep WFPC2 images to carry out a weak gravitational lensing study around 3C 324, detecting shear at the $\sim 3\sigma$ level. The conversion of this shear signal into a cluster mass depends on the unknown redshift distribution of the extremely faint ($24.5 < R < 27$) background galaxy population, but for reasonable assumptions Smail & Dickinson found that the inferred mass was compatible with an isothermal cluster potential with velocity dispersion with $700 < \sigma/\mathrm{km\ s^{-1}} < 1500$. This is consistent with the X–ray luminosity of the cluster assuming a conversion between luminosity and X–ray temperature (equivalently velocity dispersion) similar to that measured at $0 < z < 0.4$ (e.g. Edge & Stewart 1991a; Mushotzky & Scharf 1997). We return to this point in §4.3 below.

3.5. 3C 356 ($z = 1.079$):

The ROSAT PSPC and HRI observations used here were obtained by Crawford & Fabian (1993, 1996*a*), and our analysis of these data are largely consistent with theirs. 3C 356 is one of the faintest X–ray sources studied here, and the HRI exposure time is one of the shortest. The signal–to–noise is consequently somewhat poorer, making it difficult to detect extended flux from this source if it is present.

3C 356 has been the subject of extensive optical, IR and radio observation from the ground. There are two bright galaxies at $z \approx 1.08$, only 5″ apart, both approximately situated on the line connecting the widely separated radio lobes. There has been vigorous discussion about which is the true radio source host galaxy, a debate which we do not propose to join here (see Best *et al.* 1997 for a recent and comprehensive review). Both objects have compact radio components, and could therefore be AGN. Lacy & Rawlings (1994) identified two other nearby galaxies at similar redshifts, although one is redshifted by ~ 5400 km s^{-1} making its physical association with the others questionable. Wide field IR and optical images (Dickinson & Eisenhardt, in preparation) show several nearby red galaxies similar to those found around, e.g., 3C 324, but there is no strong indication of a very rich environment. 3C 356 may lie in a group or poor cluster, which would be consistent with the smaller X–ray luminosity of this system.

In our 40″ measurement aperture the X–ray flux is positive and consistent with the count rate predicted from the PSPC observation, but unfortunately is also consistent with zero at $< 1\sigma$ – the HRI background noise is too large for such a large aperture measurement to be significant. A faint, compact source is present, however, with 12.9 counts detected within an 8″ radius above an expected background of 9.4 counts – significant at $> 3\sigma$. As noted by Crawford & Fabian, the nominal position of this source (accepting the ROSAT coordinate solution as given) is closer to that of the southern of the two bright $z = 1.08$ galaxies. This object, normally called "galaxy b" by aficionados, hosts the compact flat spectrum radio component. We have centered our HRI aperture on this position. The radial profile (figure 8) and flux ratio test (figure 3) both show that it is compact and probably point–like. Crawford & Fabian find that there is no significant X–ray point source at the nominal position of the northern "galaxy a," and argue that this excludes an AGN origin for the PSPC X–ray emission. However, the HRI count rate from the faint, southern point–like component is itself consistent with the prediction based on the PSPC flux (Table 1). It is therefore difficult to state with certainty that this source is not the origin of the X–ray emission seen in the PSPC. Perhaps the best evidence for an additional, extended component is that the nominal centroid of the PSPC source is $\sim 12''$ north of the HRI position, somewhat north of galaxy "a." This is the largest discrepancy between PSPC and HRI positions among the well–detected sources studied here, and could result from additional, extended X–ray emission which is undetected in the HRI data.

It is therefore difficult to firmly establish the nature of the X–ray emission from 3C 356 with these data. Some fraction, perhaps all, of the emission may arise from a compact component, but the HRI data is also consistent with a significant extended component as proposed by Crawford & Fabian.

4. Discussion

4.1. X–ray emission from distant radio galaxies

3CR radio galaxies at $z > 1$ are among the most powerful radio sources in the universe. There are few objects at $z < 1$ with comparable radio power – among the only "local" analogs are Cygnus A ($z = 0.057$) and 3C 295 ($z = 0.461$). Both of these radio galaxies are known to inhabit moderately rich clusters (Cyg A: Spinrad & Stauffer 1982, Owen *et al.* 1997; 3C 295: Minkowski 1960; Mathieu & Spinrad 1981; Dressler & Gunn 1992) with substantial X–ray luminosities and evidence for cooling flows (Cyg A: $L_X = 6.7 \times 10^{44}$ erg s^{-1} (2–10 keV); Fabbiano *et al.* 1979, Arnaud *et al.* 1984, 1987; 3C 295: $L_X = 7.1 \times 10^{44}$ erg s^{-1} (0.5–4.5 keV); Henry *et al.* 1979, 1986). Because of its fortuitous proximity, Cygnus A has been studied in considerable detail, although its very low galactic latitude has seriously hampered optical studies of the cluster. The X–ray emission from Cygnus A is known to arise from several components. In addition to the extended cluster gas which dominates the luminosity at low energies, there is a nuclear point source whose X–ray emission is heavily absorbed (Arnaud *et al.* 1987). There is also evidence for Compton scattered X–ray emission from the radio hotspots (Harris *et al.* 1994). We must consider all of these possible emission mechanisms when examining the much less detailed X–ray data available for $z > 1$ radio galaxies.

Two of the five radio galaxies observed with the ROSAT HRI are unambiguously situated in regions of extended X–ray emission: 3C 324 and 3C 294. As discussed above, there is ample supporting evidence for the presence of a galaxy cluster around 3C 324, based on deep optical and IR imaging, spectroscopy, and a measurement of weak gravitational lensing. The angular extent of the X–ray emission from 3C 324 is much larger than that of the radio source, excluding inverse Compton processes as the emission mechanism. There can be little doubt that 3C 324 inhabits a luminous X–ray cluster. Nothing is known about the galaxy environment of 3C 294. The X–ray emission is more compact than that around 3C 324 but is still larger than the scale of the radio source, again arguing against Compton scattering as the production mechanism. Again, a hot intracluster medium is the most natural explanation for the X–ray emission. At $z = 1.786$, 3C 294 is the most distant X–ray source with clear evidence for spatial extent, and is thus arguably the most distant X–ray emitting cluster known.

Carilli *et al.* (1998a) have recently detected X–ray emission from an even more distant radio galaxy, 1138–262 at $z = 2.156$. That X–ray source is very compact in their HRI images, and they were unable to firmly establish its spatial extent. Extremely large Faraday rotation of polarized emission from the radio source, as well as its distorted radio

morphology, suggest a dense gaseous environment for 1138–262. This is similar to the situation for 3C 194 (§3.1), where the X–ray source is at best only marginally resolved by the HRI, but very large rotation measures are observed in the radio, reminiscent of systems in cooling flow environments at low redshift. Carilli *et al.* (1998b) suggest that a compact cooling flow, possibly associated with the formation of the radio galaxy, may also explain the X–ray emission from 1138–262. The X–ray data for 3C 294 and perhaps also 1138–262 offer strong encouragement that powerful radio galaxies at $z \sim 2$ may serve as useful signposts pointing to extremely distant clusters.

The X–ray source coincident with 3C 194 is very compact, perhaps point–like, and may well originate from the AGN rather than from thermal gas. As noted above, 3C 194 has the strongest flat–spectrum radio core of the five radio sources studied here, and is thus a good candidate for an object with nuclear X–ray emission. However, a strong and very compact cooling flow might also be consistent with the X–ray data, and is supported by ancillary evidence from radio observations. 3C 280 also appears to have a significant point source component, as first suggested by Worrall *et al.* (1994), but probably also has cluster emission as well – it is the one source which appears spatially extended in the PSPC images. 3C 280 has the second strongest radio core (1.2 mJy at 5 GHz; Laing, Owen & Pushell, unpublished) of the galaxies in this small sample. We cannot unambiguously settle the origin of the X–ray emission from 3C 356. An extended component may be present, as proposed by Crawford & Fabian, but the low signal–to–noise of the HRI data do not permit limits as strict as those for the other objects. There is substantial X–ray emission *within* the spatial extent of the double radio lobes of 3C 356, again ruling out inverse Compton processes.

4.2. Comparison to nearby clusters

How do these distant X–ray clusters compare to their more local counterparts? For simplicity we restrict our attention to the cases of 3C 324 and 3C 294, for which the evidence for spatial extent and the absence of any nuclear point source is clearest. Both X–ray sources have $L_X \approx 3 \times 10^{44}$ erg s^{-1} in the 1–5 keV band within a 40″ radius aperture. Our observations cannot reliably constrain the total luminosity of the clusters including flux outside the measurement radius. However, in order to be compare these objects to clusters from lower redshift samples, we may follow the same approach used to correct fluxes for those samples by adopting a standard X–ray surface brightness profile with consistent parameters. For the EMSS, Gioia *et al.* (1990) and Henry *et al.* (1992) assume that the azimuthally averaged surface brightness of clusters follow a surface brightness profile $I(\theta)$

parameterized as

$$I(\theta) = I_0[1 + (\theta/\theta_c)^2]^{-3\beta+1/2}, \quad (1)$$

where I_0 is the central surface brightness and θ_c is the angular core radius. This is the conventional form for the emission distribution from a generalized isothermal gas distribution (Cavaliere & Fusco–Fermiano 1976). The signal–to–noise of *Einstein* data used to identify the EMSS sample was generally too poor to fit the model parameters for each cluster. Henry *et al.* (1992) therefore adopted fiducial values which are typical of nearby galaxy clusters: $\beta = 2/3$ (Jones & Forman 1984) and linear core radius $r_c = D_A\theta_c = 250$ kpc, where D_A is the angular diameter distance to the cluster. This model is then used to correct for the flux outside their detection cell. For a circular aperture with angular radius θ_A the flux correction is

$$\frac{F(<\theta_A)}{F_{\rm total}} = 1 - \frac{1}{\sqrt{1 + (\theta_A/\theta_c)^2}}. \quad (2)$$

For any conventional cosmology the angular diameter distance changes very little over our redshift range $1 < z < 1.8$. Our $40''$ aperture radius therefore corresponds very nearly to a fixed metric diameter $\approx$ 340 kpc for our adopted $H_0 = 50$, $q_0 = 0.5$ world model. Thus if we use the same assumptions to correct for lost flux as were applied to the EMSS, this correction factor is then 2.4 over the entire redshift range of interest. The additional blurring of the point response function of the ROSAT PSPC results in a small increase in this correction factor for our aperture size, which we neglect given the larger measurement uncertainties in our data and those inherent in the assumption of a particular, unverified X–ray surface brightness profile. Therefore the "total" luminosities of 3C 324 and 3C 294 in the 1–5 keV band, calculated using the aperture correction assumed for the EMSS survey, would be $\sim 6 \times 10^{44}$ erg s^{-1}. The minimum luminosities (i.e. if $r_c \ll 250$ kpc) are the measured aperture values. In fact, as we will see next, the limited evidence from the X–ray images suggests that r_c is indeed smaller for our objects, ~100–150 kpc, implying somewhat smaller aperture corrections.

Our X–ray images have insufficient signal–to–noise to permit a reliable fit to the surface brightness profile and thus a direct measurement of r_c. However some simple measurements give at least a rough estimate of the angular scale of the X–ray emission, and for an assumed surface brightness profile these may be related to θ_c. An upper limit may be derived from the FWHM measured from the PSPC images, whose angular resolution, as we have seen, undersamples the X–ray emission from at least some of these clusters. Equation 1 implies $\theta_c = 0.65\times$ FWHM. Alternatively, integrating eq. 1 relates the peak surface brightness I_0 to the total flux within an aperture θ_A for a given θ_c. Measuring I_0 and $F(<\theta_A)$ thus gives us an estimate of θ_c. By comparing the peak surface brightnesses of the the PSPC and HRI

images we may get an estimate of the degree to which the X–ray emission is underresolved by the PSPC (see also below). The HRI data is noisier, to be sure, but can set a useful lower limit on θ_c – more concentrated emission would become visible as a compact source in the HRI images.

The FWHM of 3C 324 in the PSPC (figure 7) is $\sim 25''$, i.e. close to the resolution limit. Thus $\theta_c = 0.65\times$ FWHM $\approx 16''$, The S/N in the HRI image is too low to permit a direct measurement of the FWHM. The peak–to–total flux test applied to the PSPC image using data in Table 1 and figure 7, including measurement uncertainties, gives $\theta_c = 10''$ to $19''$ (1σ errors), while the noisier HRI image gives $\theta_c = 11''$ to $29''$, showing that the X–ray emission is not severely underresolved by the PSPC. We therefore take $10''$—$16''$ to be the range of acceptable θ_c values, corresponding to core radii of 85 to 140 kpc. The HRI image of 3C 294 is more compact, and the peak–to–total flux test gives $5'' < \theta_c < 14''$. The PSPC FWHM actually appears to be somewhat broader than for 3C 324, which may simply reflect noise in the images, or could imply that the compact HRI emission peaks up over a larger, underlying X–ray cluster. We adopt a range 45 – 150 for the core radius of 3C 294. The X–ray emission from these two clusters is therefore smaller than the $r_c = 250$ kpc value typical of nearby clusters in the Jones & Forman (1984) sample, and the aperture flux corrections (eq. 2) are correspondingly smaller than those computed using EMSS–style assumptions. For 3C 324 the aperture correction is in the range 1.3 to 1.6, while for 3C 294 it is 1.15 to 1.65. The total 1–5 keV luminosities of these clusters, then, would be 3 to 5×10^{44} erg s^{-1}.

To further facilitate comparison with other cluster samples, we may correct our 1–5 keV luminosities to those of more commonly used X–ray passbands. This correction will depend on the assumed spectral model. However, for energy ranges commonly used for cluster observations, the dependence on temperature is fairly weak over the range typically spanned by high luminosity clusters, $1 < kT/(1\ \mathrm{keV}) < 15$, and the dependence on metallicity for nominal ranges is weaker still. For reference, using our assumed model with $kT = 4$ keV, $Z = 0.3 \times$ cosmic abundance, the corrections to the 0.3–3.5 keV (Einstein), 0.5–2.0 keV (ROSAT hard), and 2–10 keV (EXOSAT) bandpasses are 1.22, 0.71, and 0.91, respectively. The correction to bolometric luminosity depends very little on the spectral model for this temperature range, and is 2.16 for $kT = 4$ keV. The bolometric correction increases rapidly for $kT < 1$ keV, and is nearly 10 for $kT = 0.5$ keV. Therefore if the X–rays we observe were dominated by emission from very cool gas, the total luminosity of the cluster would be many times larger than the values we derive here.

We may therefore estimate the total bolometric luminosity of the 3C 324 and 3C 294 clusters to be $L_{bol} \approx 9 \times 10^{44}$ erg/s. The dominant uncertainty is the correction to total

flux outside the measurement aperture, and is probably less than a factor of 1.5. If the gas is much cooler than 1 keV, however, the implied luminosities would be much larger. Locally, the Coma cluster has $L_{bol} = 1.6 \times 10^{45}$ erg/s (Mushotzky *et al.* 1978; Edge & Stewart 1991b). In terms of luminosity, at least, our distant clusters are broadly similar to the canonical local example, Coma. Their luminosities are also very similar to those of the Cygnus A and 3C 295 clusters. They are significantly less luminous than the brightest X–ray selected clusters at $0.5 < z < 0.8$ (Gioia & Luppino 1994). These approach 2×10^{45} erg/s (0.3–3.5 keV), compared to $\sim 5 \times 10^{44}$ erg/s in the same energy bandpass for our clusters. However, their luminosities are much greater than those of the most distant *optically* selected clusters at $z \approx 0.8$, which were studied by Castander *et al.* (1994) and found to have $L_X \lesssim 10^{44}$ erg s^{-1} in the ROSAT bandpass.

At large redshifts the cosmological $(1+z)^4$ surface brightness dimming becomes severe, and may render extended galaxy clusters difficult to detect above the instrumental and astronomical X–ray backgrounds. At the redshifts of 3C 324 and 3C 294, the diminution factors are 24 and 60, respectively. The central surface brightness of Coma as measured by Briel *et al.* (1992) from ROSAT All–Sky Survey data is 4.6×10^{-13} erg s^{-1} cm^{-2} arcmin^{-2} in the 0.5–2.4 keV band. Translating this to $z = 1.206$ and accounting for the k–correction assuming $kT = 8$ keV for Coma (the temperature adopted by Briel *et al.*), the predicted ROSAT PSPC surface brightness would be 0.0019 count s^{-1} arcmin^{-2} in the 0.4–2.4 keV observed frame bandpass. The X–ray core radius of Coma measured by Briel *et al.* is 420 kpc, so additional blurring from PSPC resolution effects would be small. The central surface brightness of 3C 324 as observed in the PSPC is ~ 0.008 count s^{-1} arcmin^{-2}, 4.2× larger than would be expected for Coma seen at that redshift. The HRI data is noisier due to the weakness of the signal from 3C 324, but the measured mean surface brightness within 6″ radius is $\sim 4.0\times$ larger than would be predicted for Coma, consistent with the PSPC data and suggesting that the cluster emission is not severely underresolved by the PSPC image. For 3C 294, the peak PSPC count rate for the Coma cluster redshifted to $z = 1.786$ would be 0.00091 count s^{-1} arcmin^{-2}, while the measured central surface brightness of 3C 294 is 3.3× higher. As can be seen from figures 1, 3 and 6, the HRI emission from 3C 294 is more centrally peaked than that of 3C 324, with a central value (again averaged within a 6″ radius) is $\sim 6.3\times$ that predicted for Coma. The PSPC image, in this case, underresolves the X–ray emission from 3C 294.

Thus while the luminosities of these high redshift systems may be similar to those of Coma, their central surface brightnesses are larger. A cluster like Coma itself, placed at these redshifts, would in fact have been difficult to detect as a source above the background in the PSPC, and would be invisible in the HRI. This illustrates the potential for surface brightness biases in detecting X–ray clusters at very high redshift. At $z > 1$, pointed

ROSAT exposures with exposure times similar to those used here might detect only those clusters with highly peaked X–ray emission, even when detection algorithms carefully designed for sensitivity to extended sources are employed.

In nearby galaxy clusters, highly peaked peaked central X–ray emission often results from the presence of a cooling flow. Abell 2597, for example, a nearby cluster with a strong central cooling flow, has a central surface brightness $\sim 30\times$ higher than that of Coma (Sarazin & McNamara 1997), and thus would easily have been detected in our ROSAT images if it were located at $1 < z < 2$, albeit perhaps as an apparent point source. The same applies to many other local cooling flow clusters with similar luminosities. Pesce *et al.* (1990) compare *Einstein* IPC surface brightness profiles for several nearby clusters with and without cooling flows – the non–cooling flow clusters have similar central surface brightnesses to that of Coma, while the cooling flow clusters peak $\sim 9\times$ higher. The high central surface brightnesses of 3C 324 and 3C 294 are suggestive but do not require the presence of cooling flows. We discuss estimates of the cooling times in §4.3 below.

Regardless of the physical origin of concentrated X–ray emission, however, ROSAT selected X–ray cluster samples could miss some significant fraction of objects at $z > 1$, even if their total luminosities are large. Moreover, as our PSPC images show, clusters like 3C 324 and 3C 294 are unlikely to be detected as *resolved* objects by any algorithm at this signal–to–noise level. They are only demonstrably extended thanks to the availability of correspondingly deep HRI images. 3C 280 appears visibly extended in the PSPC images, but such unusually deep exposures (48 ksec) are rare in the ROSAT archive. If angular extent is used as a criterion for identifying cluster sources in ROSAT PSPC images, sources like 3C 324 and 3C 294 could be excluded for this reason. One thus is in a double bind when searching for $z > 1$ clusters in PSPC data: surface brightness limits may exclude larger, resolved clusters, while angular extent requirements could eliminate compact candidates with detectably large central surface brightness. Very similar concerns (surface brightness selection effects and star/galaxy separation) have plagued observers of faint, high redshift *galaxies* for many years.

4.3. Physical Properties

Armed with nothing other than an X–ray luminosity it is difficult to reliably assess the mass of a nearby galaxy cluster nearby, not to mention one at some large redshift. To be sure L_X correlates with the virial mass of a cluster, but because the gas emission processes scale as the square of the gas density as well as with temperature the correlation is not a

simple one. The X–ray emissivity of a gas may be written as

$$L_X = \int \Lambda(T) n^2 dV \tag{3}$$

where $\Lambda(T)$ is the gas cooling function. If we express the volume integral of n^2 as $\langle n^2 \rangle V$, then for an isothermal gas distribution we may write

$$L_X = \Lambda(T) \langle n^2 \rangle V. \tag{4}$$

Similarly,

$$M_{\rm gas} = \mu m_p \langle n \rangle V \tag{5}$$

where m_p is the proton mass and μ is the mean mass per particle. The quantities $\langle n^2 \rangle$ and $\langle n \rangle^2$ are related by a geometrical factor which depends on the spatial distribution of the emitting plasma. If the distribution of the gas can be measured or a model is assumed then this proportionality can be computed. If we express the cluster volume as $V \propto R^3$ where R is some characteristic scale length (e.g. the core radius), we may therefore write

$$M_{\rm gas} \propto \left(\frac{L_X}{\Lambda(T) R^3} \right)^{1/2}. \tag{6}$$

At $T > 2 \times 10^7$K the X–ray emission from a plasma is primarily thermal Bremsstrahlung, and thus $\Lambda(T) \propto T^{1/2}$. Therefore we find

$$M_{\rm gas} \propto L_X^{1/2} T^{-1/4} R^{-3/2}. \tag{7}$$

Thus for a cluster with an observed luminosity L_X the inferred $M_{\rm gas}$ depends only weakly on the temperature (which at any rate is unknown for our distant clusters), but fairly strongly on gas density or equivalently on the cluster scale size: more concentrated, denser gas distributions require less gas mass to produce the same L_X.

Given the quality of our ROSAT data we cannot reliably measure the spatial distribution of the gas emission from these distant clusters. The β–model surface brightness profile given by equation 1 implies a density distribution

$$\rho(r) = \rho_0 [1 + (r/r_c)^2]^{-3\beta/2}, \tag{8}$$

allowing us to compute the geometrical scaling factors required above. In what follows here we will adopt this form for the density and surface brightness profile with $\beta = 2/3$ for the purpose of calculation, although the argument is generalizable.

The virial mass of a cluster scales as $M_{\rm vir} \propto T^{3/2} \rho^{-1/2}$. In an Einstein–de Sitter universe, the characteristic density of an object virialized at redshift z is proportional to the

mean background mass density at that redshift, i.e. to $\rho_c(1+z)^3$ where ρ_c is the present–day critical density. This scaling has been calibrated using local galaxy cluster samples (using masses derived variously from X–ray data, galaxy velocities, and gravitational lensing) and studied with numerical simulations by many authors (e.g. Navarro, Frenk & White 1995; Evrard, Metzler & Navarro 1996; Eke, Cole & Frenk 1996; Bryan & Norman 1998; Hjorth, Oukbir & van Kampen 1998). The redshift dependence for open or cosmological constant dominated cosmologies is a subject of ongoing investigation (Viana & Liddle 1996; Kitayama & Suto 1996; Eke, Navarro & Frenk 1998; Voit & Donahue 1998). For simplicity we restrict ourselves here to considering $\Omega_M = 1$ cosmologies. The precise scaling is unimportant for the rough exercise we perform here; we adopt that from Navarro, Frenk & White 1995:

$$M/10^{14}M_\odot = 0.87[kT/(1+z)]^{3/2} \tag{9}$$

(for $H_0 = 50$, kT in keV).

If we require for a given cluster that its gas mass be less than its total virial mass, $M_{\rm gas} < M_{\rm vir}$, then we may set a joint constraint on allowable temperatures and densities, or equivalently on temperature and size for a particular density profile. Figure 9 shows calculations[2] of $M_{\rm vir}$ and $M_{\rm gas}$ vs. temperature for the case of 3C 324 at $z = 1.206$. Here, the gas mass has been derived using an elaboration of the above arguments. The calculations are scaled to the observed 0.4–2.4 keV PSPC count rate within a 40″radius measurement aperture (Table 1). The cluster emissivity at a given temperature is determined using a redshifted Raymond & Smith (1977) model with 0.3× cosmic abundance and is used (together with the PSPC response matrix, the luminosity distance and the foreground neutral hydrogen column density) to convert the observed count rate to the emission integral over the measurement volume. The adopted surface brightness and density and profiles (eqs. 1 and 8) are then used to derive the correction to total luminosity (eq. 2), gas mass and central density for a specified r_c. Values for the central gas pressure and cooling time can then also be derived.

For 3C 324 we have the added information of a mass derived from gravitational lensing by Smail & Dickinson (1995) (see §3.4). The precise value of this mass is quite uncertain both because the signal from the lensing shear is weak and the redshift distribution of the very faint galaxies used to make the measurement is unknown. However a fairly robust minimum mass of a few $\times 10^{14}M_\odot$ can be inferred from the very existence of a lensing signal.

---

[2]Note that the Hubble Constant dependencies of the two masses are different: $M_{\rm vir} \propto h^{-1}$ while $M_{\rm gas}$ is approximately $\propto h^{-2.5}$. The latter scaling is exact if $\theta_c \ll 40''$ but deviates from this proportionality for large core radii where the correction for flux outside the measurement aperture becomes large. In this case the h^{-1} scaling of core radius with angular diameter becomes dominant.

The dashed lines in figure 9 show the allowable mass range derived by Smail & Dickinson (1995) assuming that 25–75% of galaxies with $24.5 < R < 27$ (the lensed population) lie beyond $z = 1.2$, and including the uncertainty on the tangential shear measurement. The computed masses are computed within a 500 kpc radius and assume a spherical isothermal potential. The lensing masses intersect the predicted virial mass (eq. 9) for $kT = 8^{+12}_{-4.5}$ keV. Temperatures $\ll 3$ keV would be very unlikely if the $M_{\rm vir}$ vs. T relation predicted by eq. 9 has any validity.

While $M_{\rm vir}$ depends strongly on temperature, $M_{\rm gas}$ depends primarily on gas density, or as plotted in figure 9, on the X–ray core radius. For a given temperature, the mean squared gas density has a minimum value (or the core radius a maximum, for the adopted density model) in order that $M_{\rm gas} < M_{\rm vir}$. Presumably the real gas mass fraction is lower – in nearby clusters this value is more typically in the range $10\text{–}30h_{50}^{-3/2}\%$ (Briel *et al.* 1992; White *et al.* 1993; White & Fabian 1995; Hughes 1998), a value which has proven difficult to reconcile with the cosmic baryon density predicted by Big Bang nucleosynthesis for $\Omega_M = 1$ world models. Therefore we also plot a line for $0.15M_{vir}$ in figure 9, the mean value (measured within a 1 Mpc radius) for nearby rich clusters (White & Fabian 1995).

If we assume that the gas is at the virial temperature of the cluster, then for a given temperature we may evaluate the maximum X–ray core radius which is consistent with a specified gas mass fraction. In figure 10 (upper left panel) we show this maximum core radius vs. kT for 3C 324 for the assumptions $M_{\rm gas}/M_{\rm vir} = 1$ or 0.15. The approximate temperature range implied by the lensing constraints on $M_{\rm vir}$ is indicated, as are the bounds on r_c derived from the image analysis above. The derived values of r_c are barely consistent with these constraints for the low end of the temperature range and/or for gas mass fractions < 0.15. If this analysis is valid, then the temperature of the 3C 324 X–ray gas should be approximately 4 keV unless the minimum lensing mass is an overestimate or the core radius were larger than our proposed upper limit. Also shown in figure 10 are the central densities, pressures, and cooling times computed from the same models. The cooling time for $M_{\rm gas}/M_{\rm vir} = 0.15$ is less than the age of the universe at $z = 1.21$ for $kT < 5.5$ keV, and can be as short as 1.8 Gyr if $kT = 3.5$. It is therefore plausible, if not required, that the clusters hosting these radio galaxies have central cooling flows.

Similar constraints apply to 3C 294 (figure 11). At $z = 1.8$ the mass appropriate to a given virial temperature (eq. 9) should be smaller. Because the X–ray luminosity of 3C 294 is similar to that of 3C 324, the gas must therefore be somewhat denser at a given temperature unless the gas mass fraction is larger. Indeed the X–ray emission from 3C 294 is more compact than that of 3C 324, so this constraint is satisfied. For a gas mass fraction of 0.15, the implied cooling time is shorter than the age of the universe at $z = 1.8$ for any

temperature $kT < 7$ keV.

Other properties of FR II radio sources have been used to derive information about their gaseous environments. Wellman, Daly & Wan (1997) have studied a sample of 3CR radio sources (both radio galaxies and quasars) at $0 < z < 2$, deriving the density of the ambient medium from an analysis of lobe propagation velocities and minimum energy magnetic fields which can be derived from radio maps (see also Daly 1995 and Wan & Daly 1996). They find that FR II sources are typically found in gaseous environments similar to those of nearby galaxy clusters – their analysis includes Cygnus A, where the parameters derived from the radio data may be compared with X–ray observations of the intracluster medium (ICM). There is some suggestion in their data that the ICM pressures and densities are lower at $z > 1$ than they are for similar radio sources locally, with $n \sim 0.002 h_{50}^{1/2}$ being the typical value they derive for their high redshift sample. This is 5–20× lower than the central density we derive for the 3C 324 ICM, and 3C 294 seems to be in a still denser environment. We require such large gas densities in order to produce the observed X–ray luminosities from a cluster whose gas mass does not exceed the virial mass predicted by equation 9. If, however, equation 9 does not accurately describe the mass–temperature relation at high redshift, then larger gas (and total) masses might be allowed which would be consistent with the densities derived by the radio source analysis. Such might be the case in an open universe, where the characteristic mass scale for structure formation evolves more slowly than in the Einstein–de Sitter cosmology. Unfortunately the radio galaxy sample analyzed by Wellman *et al.* does not include 3C 324 or 3C 294. A similar investigation of the ambient density derived from the radio data on those objects would offer an interesting test of these models.

4.4. Space densities

Ultimately, we would like to use observations of high redshift clusters to place constraints on the spectrum of mass fluctuations in the universe, on the evolution of the intracluster medium, and on the cosmological geometry. For this reason, many observers have carried out surveys of distant, X–ray selected clusters, in order to measure their luminosity function and temperatures at high redshifts. Theory, however, provides only straightforward predictions for the evolution of the cluster *mass* function. The X–ray observables (e.g. luminosity, temperature) must then be related to the underlying cluster masses. This relation depends on the evolution of the intracluster medium, however, and is not straightforward to predict.

In hierarchical models of structure formation by gravitational instability, the evolution

of the cluster mass function $n(M, z)$, the number density of clusters with a given mass at a given redshift, is highly sensitive to the shape and normalization of the power spectrum, and to the cosmological geometry. This evolution is believed to be well described by the analytical formalism of Press & Schechter (1974), which has been tested extensively and verified on cluster mass scales by N–body experiments (cf. Eke *et al.* 1996, Borgani *et al.* 1998). For a fixed cosmology and a power spectrum normalized to local ($z = 0$) constraints, the redshift evolution of the mass function is extremely rapid for $\Omega_M = 1$ but less so for Λ–dominated and especially for open universes (e.g. Eke *et al.* 1996, Viana & Liddle 1996, Bahcall *et al.* 1997). The growth of structure "freezes out" at redshift $z \approx 1./(\Omega_0^{-1} - 1)$ in open universes and cluster evolution slows down, while it progresses continually at all redshifts for $\Omega_0 = 1$ cosmologies.

The evolution expected in an $\Omega_M = 1$, $\Lambda = 0$ cosmology is so rapid that at very large redshift the existence of only a few massive clusters would pose a serious problem (cf. Donahue *et al.* 1998; Bahcall, Fan & Cen 1997; Eke et al. 1998). For a CDM–like power spectrum normalized at the cluster mass scale using local cluster constraints ($\sigma_8 = 0.50\Omega_0^{-0.47+0.1\Omega_0}$; Eke *et al.* 1996), the Press–Schechter formula predicts that in an Einstein–de Sitter universe, clusters with mass $2 \times 10^{44} M_\odot$ (near the lower limit to the lensing mass derived for 3C 324) should be 2000× less common at $z = 1.206$ than locally, and 900000× less common at $z = 1.786$. The evolution of higher mass clusters is more rapid still.[3] At $z \approx 1.8$ they are sufficiently rare that dN/dz, the number of such clusters per unit redshift found over *the entire sky,* is ~ 1. In an open universe or one dominated by a cosmological constant, clusters would be much more common at these redshifts: ~ 30 and 1000× more abundant at $z = 1.2$ and $z = 1.8$, respectively, for $\Omega_M = 0.35$ versus $\Omega_M = 1$.

Unfortunately, we do not yet have any direct measurement of the mass for 3C 294 – a total mass $\lesssim 10^{14} M_\odot$ is still compatible with the existing data. For 3C 324, the gravitational lensing measurement provides at least a rough lower limit for the mass. Without X–ray data of outstanding quality, it is difficult or impossible to go from the observables for a given cluster to its total mass. As a minimum we require data on the luminosity, temperature and surface brightness profile of the cluster. For the $z > 1$ clusters discussed here, the existing ROSAT data provides only an measure of the luminosity. It is already clear from existing, comprehensive surveys for X–ray clusters at $z < 1$ that X–ray luminosity cannot scale simply with the mass at all redshifts. The X–ray luminosity function evolves very little out to $z = 0.8$ at the luminosities of interest here (Rosati *et al.* 1998, Scharf *et al.* 1997, Collins *et al.*), and there is little evidence for strong evolution

[3]For comparison, the mass of Coma within a radius of 1 Mpc is approximately $6 \times 10^{14} M_\odot$, and its total mass may be $\sim 2\times$ larger (Hughes 1998).

in the luminosity–temperature relation out to at least $z \approx 0.4$ (Mushotzky & Scharf 1997; Henry 1997) and perhaps beyond (Donahue *et al.* 1998). Therefore X–ray emission is related to cluster mass in a more complicated fashion, presumably due to the evolutionary history of the intracluster medium. Understanding this evolution is a currently an active field of exploration both observationally and theoretically.

The fact that our clusters are selected from a survey targeting powerful radio sources makes it difficult to provide a good estimate of the space density of massive clusters at $z > 1$. We are observing a special subset of clusters, those with powerful radio sources, and cannot readily extrapolate to the cluster population as a whole at that redshift. However, even lower limits are interesting for comparison to some models (particularly, as noted above, if more robust mass estimates could be assigned). Two representative numbers may be derived from our data if we make the maximally conservative assumption that the *only* galaxy clusters which exist at $z > 1$ are those which host powerful radio galaxies. The 3CR radio survey from which our targets were drawn covers approximately 14000 deg^2 of the sky, and has nearly complete redshift identification. There are 34 radio galaxies with $1 < z < 2$ in this survey. Of these, we know that at least two have extended X–ray emission with flux $> 10^{-14}$ erg s^{-1} cm^{-2} in the ROSAT bandpass, setting a minimum surface density on the sky of 0.46 steradian^{-1}. If we instead assume that 4 out of 5 of our radio galaxies are situated in X–ray clusters (i.e. excluding only 3C 194), and that this proportion can be extended to the whole 3CR sample of 34 galaxies, the surface density would be 6.2 steradian^{-1}.

We may compare this to an early prediction for cluster observations with ROSAT made by Evrard & Henry (1991). They employed the Press–Schechter formalism in an Einstein–de Sitter universe for models with various power spectrum parameters, and tested various models for the evolution of the intracluster gas in order to calculate X–ray fluxes in the ROSAT bandpasses. In particular, two of their models, which they label "CDMP3" and "XCDM," are broadly consistent the EMSS determination of the X–ray luminosity function at $0 < z < 0.5$, and with the weak evolution of the luminosity–temperature relation over the same redshift range. The XCDM model in particular maintains a minimum entropy for the intracluster medium, a scenario which has been invoked to explain the slope and lack of strong evolution in the luminosity–temperature relation (see also Kaiser 1991; Henry 1997; Mushotzky & Scharf 1997). Evrard & Henry calculate predictions for the number of clusters detectable with flux $> 10^{-14}$ erg s^{-1} cm^{-2} and $z > 1$: their values are 18 and 5.3 steradian^{-1} for the two models respectively. If anything, their models overpredict the number counts of cluster X–ray sources at fluxes of 10^{-14} erg s^{-1} cm^{-2} when compared to the observations of Rosati *et al.* 1995. Thus the minimum number densities derived from our radio galaxy clusters do not robustly constrain these models. However presumably there may be many

more clusters at similar redshifts *without* powerful FR II radio sources. If $\lesssim 10\%$ of rich clusters at $z > 1$ host powerful radio galaxies, then these simple $\Omega = 1$ models would be inconsistent with the data. The detection of a cluster at $z = 1.27$ by Stanford *et al.* 1997, evidently an X–ray source with $L_X \approx 1.5 \times 10^{44}$ erg s^{-1}, is particularly important in this regard. This cluster was found in a "blind" infrared search of merely 100 arcmin^2. Naively, this implies a surface density of 10^5 steradian$^{-}1$ for such objects – enormously exceeding expectations from the Evrard & Henry models. It will be extremely important to verify the X–ray and mass properties of that cluster and to search for more like it.

Finally, we note the importance of determining a reliable mass for at least one galaxy cluster at $z \approx 2$. In an Einstein–de Sitter cosmology with hierarchical structure formation, there should be essentially no virialized clusters in the universe at such a redshift with $M > 10^{14} M_\odot$. The existence of even one would be a powerful constraint on such world models.

5. Conclusions

It is clear that powerful radio galaxies at least sometimes provide good markers of deep gravitational potential wells at high redshift. In this regard they may even more useful than clusters identified than do faint galaxy enhancements identified in optical images, as many of these at $z \sim 0.8$ have been found to have rather low X–ray luminosities (Castander *et al.* 1995). Analogies have often been drawn between powerful radio galaxies and brightest cluster ellipticals or cD galaxies (e.g. Kristian, Sandage & Katem 1978; Lebofsky & Eisenhardt 1986; Best *et al.* 1998*a*.). There is good evidence that powerful FR II radio sources trace a population of massive galaxies formed at high redshift. In hierarchical clustering theories, where most galaxy assembly takes place over an extended range of redshifts, early formation of massive galaxies is a relatively rare event involving highly biased peaks in the matter distribution, and takes place only in unusually overdense regions of the space. These are thus most likely to mark the cites of early cluster formation in the universe. It has been suggested (cf. Fabian *et al.* 1986; Fabian 1989) that distant radio galaxies and quasars may be situated in massive cooling flows, and perhaps may even be forming due to the conversion of the mass flow into stars. If so, these cooling flows may contribute substantially to their X–ray luminosity and enhance their surface brightness (and hence detectability) in ROSAT images.

These data leave little doubt that clusters with substantial X–ray luminosities, similar to "L_X^*" clusters in the local universe, do exist beyond a redshift of unity. Given the extremely sparse nature of the X–ray data now available, detailed comparison between the

properties of intracluster medium and those of nearby clusters must await observations with future X–ray observatories. In addition, the targeted nature of the present survey makes it difficult to provide any useful constraint on the space density of X–ray clusters at $z > 1$. Clearly, a more systematic survey without restriction to radio sources would be more useful for constraining their space density. This, however, will be extremely challenging. The surface density of such clusters on the sky is expected to be quite low for any standard model, requiring very deep X–ray data over a very large solid angle to detect even a few clusters. The XMM mission, with its large collecting area and correspondingly deep flux sensitivity, offers the opportunity to do this. However, even then the X–ray source selection strategy must be considered carefully; XMM will have an angular resolution similar to that of the ROSAT PSPC, and therefore clusters like the ones presented here may appear to be unresolved and thus hard to distinguish from the much more numerous point–like AGN sources at these fluxes. Also, as we have discussed, imaging and spectroscopic follow–up of clusters at $z > 1$ is challenging even with 8 to 10 meter class telescopes, but it is feasible.

The radio galaxy selection strategy may therefore still have a useful role in the future, as a means of enormously restricting the survey area to fields where cluster emission is likely, and where the probable redshift is known *a priori*. By extending an X–ray survey of high redshift radio galaxies to study the much more numerous objects with radio fluxes fainter those of the 3CR, and by robustly quantifying the fraction of such radio galaxies which are situated in extended X–ray atmospheres, one might increase the derived lower limit to the cluster density at $1 < z < 2$ to a level where it can seriously constrain the evolutionary models. While this approach would miss the clusters *without* powerful radio galaxies, the savings in telescope time both for the X–ray observations and the ground–based follow–up could be large enough to make it the most practical method to build an interestingly large sample in a short time.

Detailed measurements of the properties of the X–ray emitting gas from clusters at $z > 1$ would also be invaluable in order to derive temperatures, ICM metallicities, total and gas masses, central gas densities, and cooling times. X–ray spectroscopy of clusters at these flux levels should be possible with XMM and can provide temperature measurements and perhaps metallicities, while AXAF can readily provide images with sufficient angular resolution and signal–to–noise to measure the spatial distribution of the X–ray emitting gas. Without such information we can do little to compare the physical properties of these distant clusters to those of their nearby counterparts.

Observing the detailed properties of even a few massive clusters at $1 < z < 2$, when the universe was only a few billion years old, could provide important clues about to the formation and early evolutionary history of the most massive structures. Just as the recent

explosion of data on high redshift galaxies has provided observational cosmology with its first direct data on the formation and early history of galaxies, observations of clusters in that early cosmic time frame can set the strongest constraints on models for structure formation, on the history of galaxy formation and metal ejection within those structures, and on the parameters of the cosmological model itself.

MD wishes to thank Dan Harris and Kim Weaver for assistance with the PROS and XSPEC software, respectively; Piero Rosati for useful information and many interesting discussions; and the various ROSAT time allocation committees throughout the years who have supported our requests for so many kiloseconds needed to gather so few high–z photons. We would also like to thank George Djorgovski for his involvement with the early stages of this project. This work was partially supported by NASA ROSAT grant NAG–3209.

REFERENCES

Allington–Smith, J.R., Ellis, R., Zirbel, E.L., & Oemler. A., 1993, ApJ, 404, 521

Aragón–Salamanca, A., Ellis, R.S., Couch, W.J., and Carter, D., 1993, MNRAS, 248, 128

Arnaud, K.A., 1996, in *Astronomical Data Analysis Software and Systems V,* eds. G. Jacoby & J. Barnes, (ASP: San Francisco)

Arnaud, K.A., Fabian, A.C., Eales, S.A., Jones, C., & Forman, W., 1984, MNRAS, 211, 981

Arnaud, K.A., Johnstone, R.M., Fabian, A.C., Crawford, C.S., Nulsen, P.E.J., Shafer, R.A., & Mushotzky, R.F., 1987, 227, 241.

Bahcall, N.A., Fan, X., & Cen, R., 1997, ApJ, 485, L53

Best, P.N., Longair, M.S., & Röttgering, H.J.A., 1997, MNRAS, 292, 758

Best, P.N., Longair, M.S., & Röttgering, H.J.A., 1998*a*, MNRAS, in press (astro-ph/9709195)

Best, P.N., Carilli, C.L., Garrington, S.T., Longair, M.S., & Röttgering, H.J.A., 1998*b*, MNRAS, in press (astro-ph/9803130)

Borgani, S., Rosati, P., Tozzi, P., & Norman, C., 1998, ApJ, submitted

Briel, U.G., Henry, J.P., & Böhringer, H., 1992, å, 259, L31

Bryan, G.L., & Norman, M.L., 1998, ApJ, 495, 80

Butcher, H. & Oemler, A., Jr. 1978, ApJ, 219, 18

Carilli, C.L., Harris, D.E., Pentericci, L., Röttgering, H.J.A., Miley, G.K., & Bremer, M.N., 1998a, ApJ, 494, L143.

Carilli, C.L., Harris, D.E., Pentericci, L., Röttgering, H.J.A., Miley, G.K., & Bremer, M.N., 1998b, ApJ, 496, L57.

Castander, F.J., Ellis, R.S., Frenk, C.S., Dressler, A., & Gunn, J.E., 1994, ApJ, 424, L79

Castander, F.J., Bower, R.G., Ellis, R.S., Aragón–Salamanca, A., Mason, K.O., Hasinger, G., McMahon, R.G., Carrera, F.J., Mittaz, J.P.D., Perez–Fournon, I., & Lehto, H.J., 1995, Nature, 377, 39

Cavaliere, A., & Fusco–Femiano, R., 1976, å, 49, 137

Collins, C.A., Burke, D.J., Romer, A.K., Sharples, R.M., & Nichol, R.C., 1997, ApJ, 479, L117

Couch, W.J., Ellis, R.S., MacLaren, I., & Malin, D.F., 1991, MNRAS, 249, 606

Crawford, C.S., & Fabian, A.C., 1993, MNRAS, 260, L15

Crawford, C.S., & Fabian, A.C., 1995, MNRAS, 273, 827

Crawford, C.S., & Fabian, A.C., 1996*a*, MNRAS, 281, L5

Crawford, C.S., & Fabian, A.C., 1996*b*, MNRAS, 282, 1483

Daly, R.A., 1995, ApJ, 454, 580

David, L.P., Harnden, F.R., Kearns, K.E., Zombeck, M.V., 1997, *The ROSAT High Resolution Imager (HRI) Calibration Report,* U.S. ROSAT Science Data Center/SAO

Dickinson, M. 1994, Ph.D. thesis, U.C. Berkeley

Dickinson, M., 1995*a*, in *Galaxies in the Young Universe,* eds. H. Hippelein, K. Meisenheimer, & H.-J. Roser, (Springer: Berlin), p. 144

Dickinson, M. 1995*b*, in *Fresh Views of Elliptical Galaxies,* eds. A. Buzzoni, A. Renzini, & A. Serrano, (ASP: San Francisco), p. 283

Dickinson, M. 1997*a*, in *The Early Universe with the VLT,* ed. J. Bergeron, (Springer: Berlin), p. 274

Dickinson, M. 1997*b*, in *HST and the High Redshift Universe,* eds. N. Tanvir, A. Aragón-Salamanca, and J.V. Wall, World Scientific, p. 207.

Dickinson, M. 1997*c*, in *Galaxy Scaling Relations: Origins, Evolution and Applications,* eds. L. da Costa & A. Renzini, (Springer: Berlin), p. 215.

Djorgovski, S., Spinrad, H., McCarthy, P., Dickinson, M., van Breugel, W., & Strom, R.G., 1988, AJ, 96, 836

Donahue, M., Voit, G.M., Gioia, I., Luppino, G., Hughes, J.P., & Stocke, J.T., 1998, ApJ, in press

Dressler, A., & Gunn, J. 1992, ApJS, 78, 1

Edge, A.C., & Stewart, G.C., 1991a, MNRAS, 252, 414

Edge, A.C., & Stewart, G.C., 1991b, MNRAS, 252, 428

Eke, V.R., Cole, S., & Frenk, C.S., 1996, MNRAS, 282, 263

Eke, V.R., Navarro, J.F., & Frenk, C.S., 1998, ApJ, in press

Eke, V.R., Cole, S., Frenk, C.S., & Henry, J.P., 1998, MNRAS, submitted

Ellis, R.S., Smail, I., Dressler, A., Couch, W.J., Oemler, A., Butcher, H., & Sharples, R.M., 1997, ApJ, 483, 582

Evrard, A.E., & Henry, J.P., 1991, ApJ, 383, 95

Evrard, A.E., Metzler, C.A., & Navarro, J.F., 1996, ApJ, 469, 494

Fabian, A.C., Arnaud, K.A., Nulsen, P.E.J., & Mushotzky, R.F., 1986, ApJ, 305, 9

Fabian, A.C., 1989, MNRAS, 238, 41P

Fabbiano, G., Schwartz, D.A., Schwarz, J., Doxsey, R.E., & Johnston, M., 1979, ApJ, 230, L67

Fabbiano, G., Miller, L., Trinchieri, G., Longair, M., & Elvis, M., 1984, ApJ, 277, 115

Feigelson, E.D., & Berg, C.J. 1983, ApJ, 269, 400.

Gioia, I.M., Maccacaro, T., Schild, R.E., Wolter, A., & Stocke, J.T., 1990, ApJS, 72, 567.

Gioia, I.M., & Luppino, G.A., 1994, ApJS, 94, 583

Gunn, J.E., Hoessel, J.G., and Oke, J.B. 1986, ApJ, 306, 30

Harris, D.E., Carilli, C.L., & Perley, R.A., 1994, Nature, 367, 713.

Hattori, K., Ikebe, Y., Asaoka, I., Takeshima, T., Boehringer, H., Mihara, T., Neumann, D.M., Schindler, S., Tsuru, T., Tamura, T., 1997, Nature, 388, 146

Henry, J.P., Branduardi, G., Briel, U., Fabricant, D., Feigelson, E., Murray, S., Soltan, A., & Tananbaum, H., 1979, ApJ, 234, L15

Henry, J.P., & Henriksen, M.J., 1986, ApJ, 301, 689.

Henry, J.P., Gioia, I.M., Maccacaro, T., Morris, S.L., Stocke, J.T., & Wolter, A., 1992, ApJ, 386, 408

Henry, J.P., Gioia, I.M., Mullis, C.R., Clowe, D.I., Lupino, G.A., Boehringer, H., Briel, U.G., Voges, W., & Huchra, J.P., 1997, AJ, 114, 1293

Henry, J.P., 1997, ApJ, 489, L1

Hill, G.J., and Lilly, S.J. 1991, ApJ, 367, 1

Hjorth, J., Oukbir, J., & van Kampen, E., 1998, MNRAS, in press

Hughes, J.P., 1998, in *Untangling Coma Berenices: A New Vision of an Old Cluster*, eds. A. Mazure, F. Casoli, F. Durret, & D. Gerbal, World Scientific, p 175

Jones, C.J., and Forman, W.R., 1984, ApJ, 276, 38

Kaiser, N., 1991, ApJ, 383, 104

Kitayama, T., & Suto, Y., 1996, ApJ, 469, 480

Kristian, J., Sandage, A., & Katem, B., 1978, ApJ, 219, 803

Lacy, M., & Rawlings, S., 1994, MNRAS, 270, 431

Lebofsky, M.J., & Eisenhardt, P.R.M., 1986, ApJ, 300, 151

Mathieu, R.D., & Spinrad, H., 1981, ApJ, 251, 485

McCarthy, P.J., Spinrad, H., van Breugel, W., Liebert, J., Dickinson, M., Djorgovski, S., & Eisenhardt, P., 1990, ApJ, 365, 487

Minkowski, R., 1960, ApJ, 132, 908

Mushotzky, R.F., Serlemitsos, P.J., Smith, B.W., Boldt, E.A., and Holt, S.S., 1978, 225, 21

Mushotzky, R.F., & Scharf, C.A., 1997, ApJ, 482, L13

Navarro, J.F., Frenk, C.S., & White, S.D.M., 1995, MNRAS, 275, 720

Owen, F.N., Ledlow, M.J., Morrison, G.E., & Hill, J.M., 1997, ApJ, 488, L15

Pedelty, J.A., Rudnick, L., McCarthy, P.J., & Spinrad, H., 1989, AJ, 97, 647

Pesce, J.E., Fabian, A.C., Edge, A.C., & Johnstone, R.M., 1990, MNRAS, 244, 58

Postman, M., Lubin, L.M., Gunn, J.E., Oke, J.B., Hoessel, J.G., Schneider, D.P., & Christensen, J.A., 1996, AJ, 111, 615

Press, W.H., & Schechter, P., 1974, ApJ, 187, 425

Raymond, J.C., and Smith, B.W., 1977, ApJS, 35, 419

Rosati, P., Della Ceca, R., Burg, R., Norman, C., & Giacconi, R., 1995, ApJ, 445, L11

Rosati, P., Della Ceca, R., Norman, C., & Giacconi, R., 1998, ApJ, 492, L21

Sarazin, C.L., & McNamara, B.R., 1997, ApJ, 480, 203

Scharf, C.A., Jones, L.R., Ebeling, H., Perlman, E., Malkan, M., & Wegner, G., 1997, ApJ, 477, 79

Smail, I., and Dickinson, M. 1995, ApJ, 455, L99

Spinrad, H., & Stauffer, J.R., 1982, MNRAS, 200, 153

Stanford, S.A., Elston, R., Eisenhardt, P., Spinrad, H., Stern, D., & Dey, A., 1997, AJ, 114, 2232

Stanford, S.A., Eisenhardt, P., & Dickinson, M., 1998, ApJ, 492, 461

Stark, A.A., Gammie, C.F., Wilson, R.W., Bally, J., Linke, R.A., Heiles, C. & Hurwitz, M., 1992, ApJS, 79, 77

Stewart, G.C., Fabian, A.C., Jones, C., & Forman, W., 1984, ApJ, 285, 1.

Strom, R.G., Riley, J.M., Spinrad, H., van Breugel, W.J.M., Djorgovski, S., Liebert, J., & McCarthy, P.J., 1990, å, 227, 19

Taylor, G.B., Inoue, M., & Tabara, H., 1992, å, 264, 415

Taylor, G.B., Barton, E.J., & Ge, J., 1994, AJ, 107, 1942

van Dokkum, P. & Franx, M. 1996, MNRAS, 281, 985

Viana, P.T.P., & Liddle, A.W., 1996, MNRAS, 281, 323

Voit, G.M., & Donahue, M., 1998, ApJ, submitted

Wan, L., & Daly, R.A., 1996, ApJ, 467, 145

Wellman, G.F., Daly, R.A., & Wan, L., 1997, ApJ, 480, 96.

White, D.A., & Fabian, A.C., 1995, MNRAS, 273, 72

White. S.D.M., Navarro, J.F., Evrard, A.E., & Frenk, C.S., 1993, Nature, 366, 429

Worrall, D.M., Lawrence, C.R., Pearson, T.J., Readhead, A.C.S., 1994, ApJ, 420, L17.

Viana, P.T.P., & Liddle, A.R., MNRAS, 281, 531L

Vikhlinin, A., McNamara, B.R., Forman, W., Jones, C., Quintana, H., & Hornstrup, A., 1998, ApJ, in press

Yates, M., Miller, L., and Peacock, J. 1989, MNRAS, 240, 129

Yee, H.K.C., and Green, R.F. 1984, ApJ, 280, 79

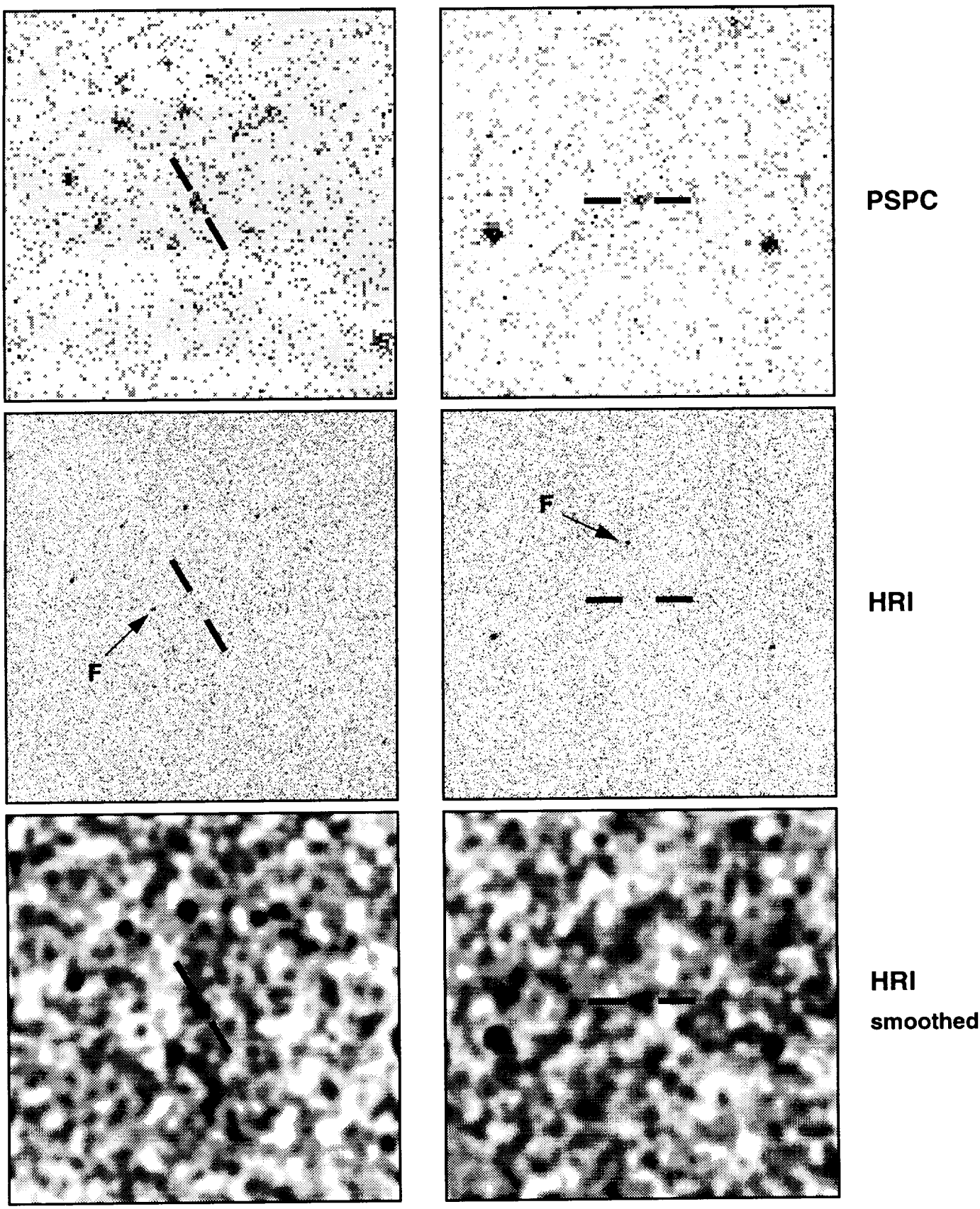
3C 294 z = 1.786
3C 324 z = 1.206
PSPC
HRI
HRI
smoothed
F
F

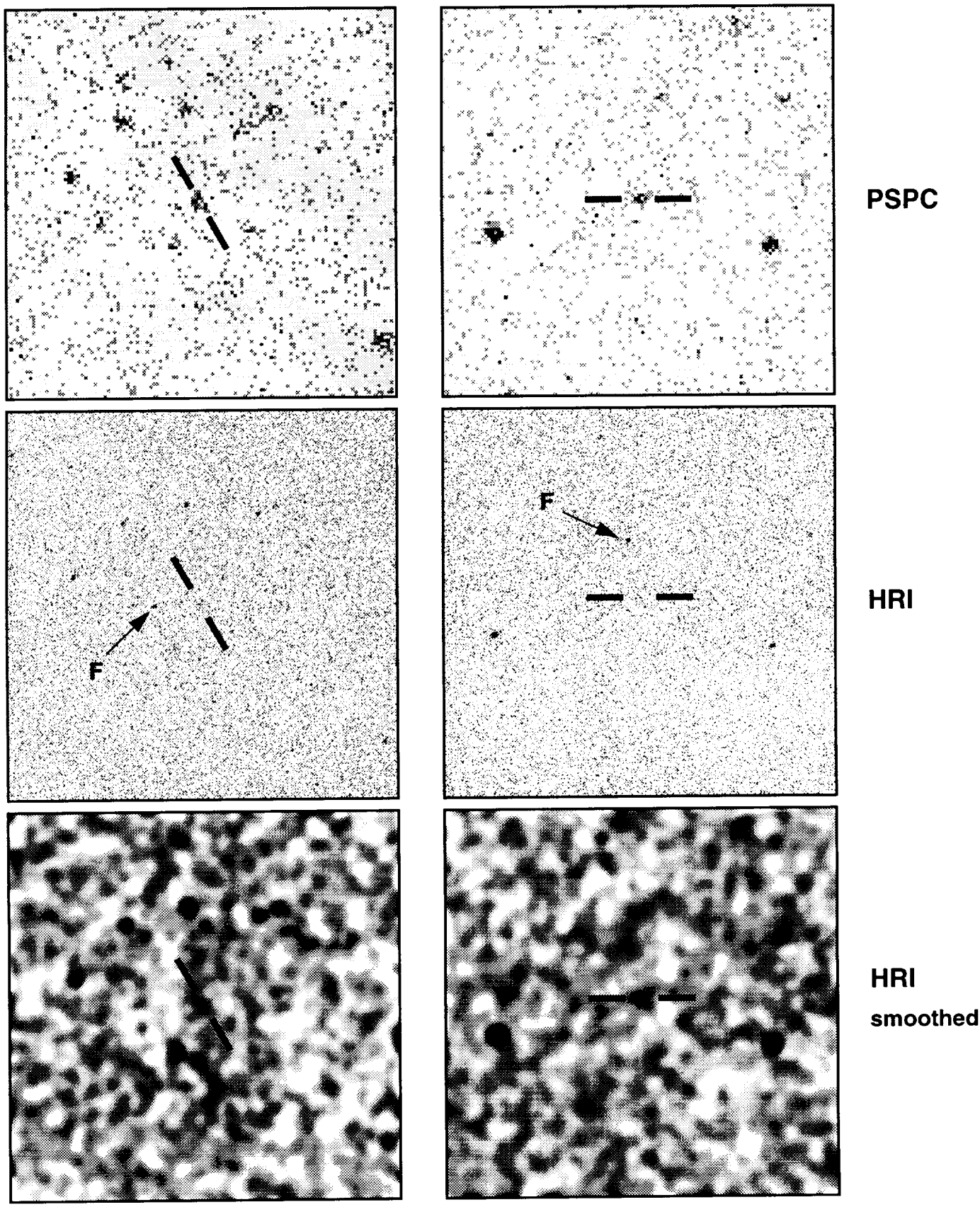
3C 294 z = 1.786
3C 324 z = 1.206
PSPC
HRI
HRI
smoothed
F
F

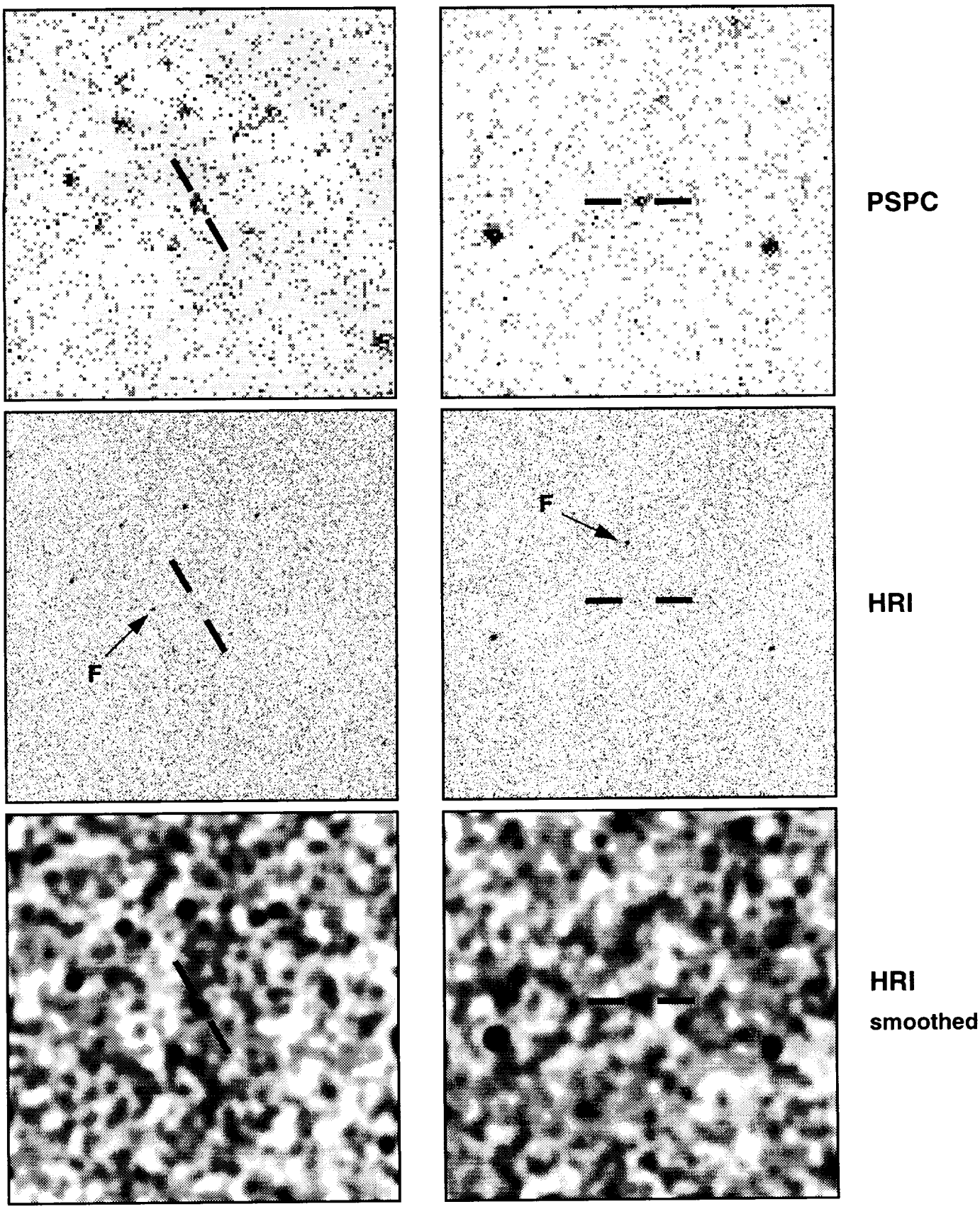
3C 294 z = 1.786
3C 324 z = 1.206
F
F
PSPC
HRI
HRI
smoothed

Fig. 1.— (Plate X) ROSAT images of four radio galaxies at $z \gtrsim 1$. (Plate X) ROSAT images of four radio galaxies at $z \gtrsim 1$. The field of view for each panel is 16 arcminutes on a side, with north up and east left. For each object the 0.4–2.4 keV PSPC image is shown at top, with the source corresponding to the radio galaxy marked. The HRI images are shown in the central panel. In each of these, an artificial point source has been added (marked "F") with the appropriate flux derived from the PSPC measurements, as described in the text. In most fields, additional point sources are also visible – these provide a useful visual comparison to the source (or lack thereof) at the position of the radio galaxy. At bottom, the HRI image is shown after convolution with a Gaussian kernel with FWHM = 30″, i.e. to an effective angular resolution similar to that of the PSPC data.

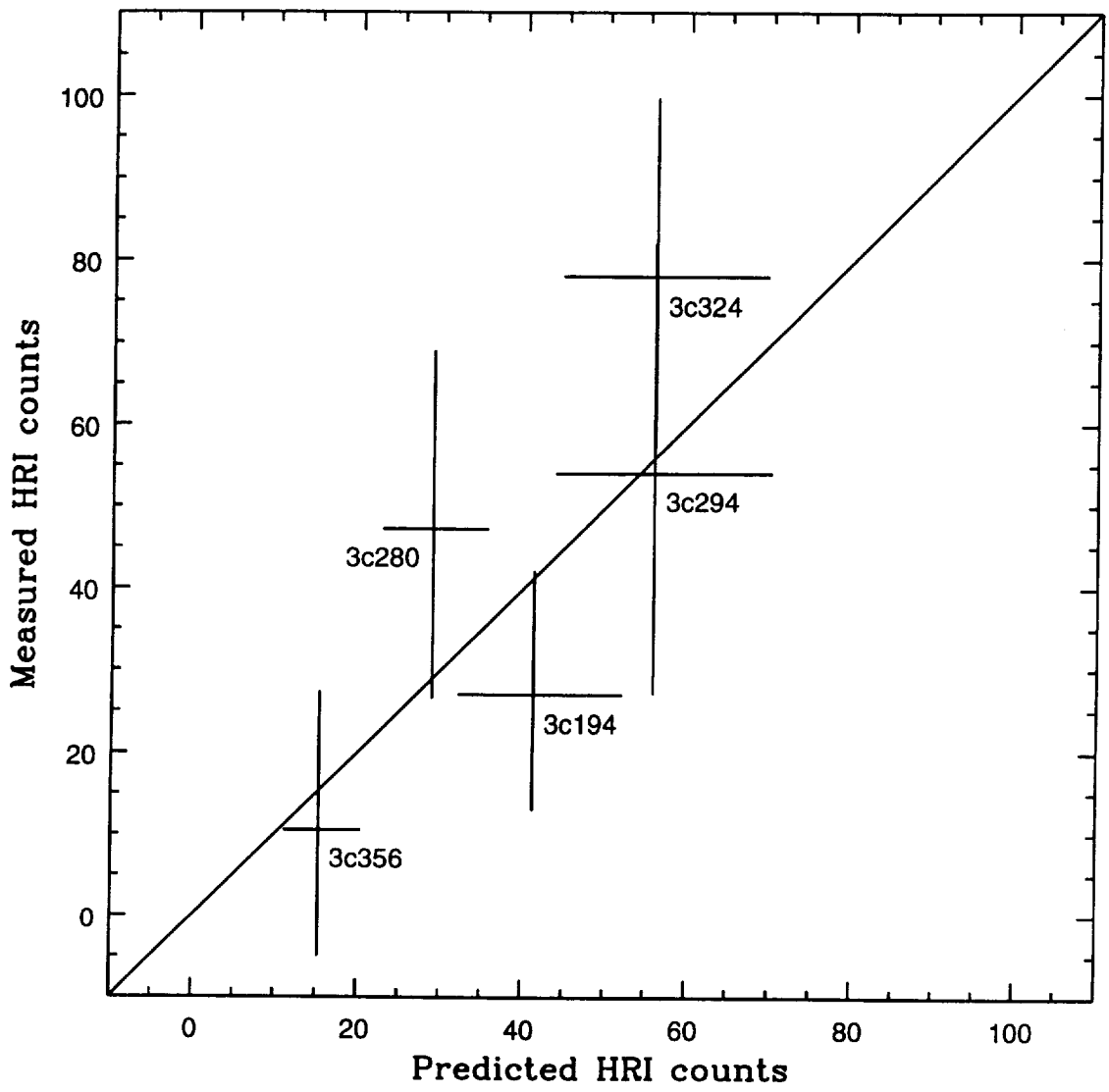

Fig. 2.— Comparison of the predicted and measured HRI fluxes (expressed as total detected photon counts) within an 40″ radius aperture for the five radio galaxies studied here. The predicted count rates are based on the flux measured from the PSPC data, converted to HRI count rates using an assumed thermal model for the X–ray emission (see text and Table 1). Although the individual HRI detections have low formal significance they are all positive and consistent with the fluxes measured by the PSPC observations.

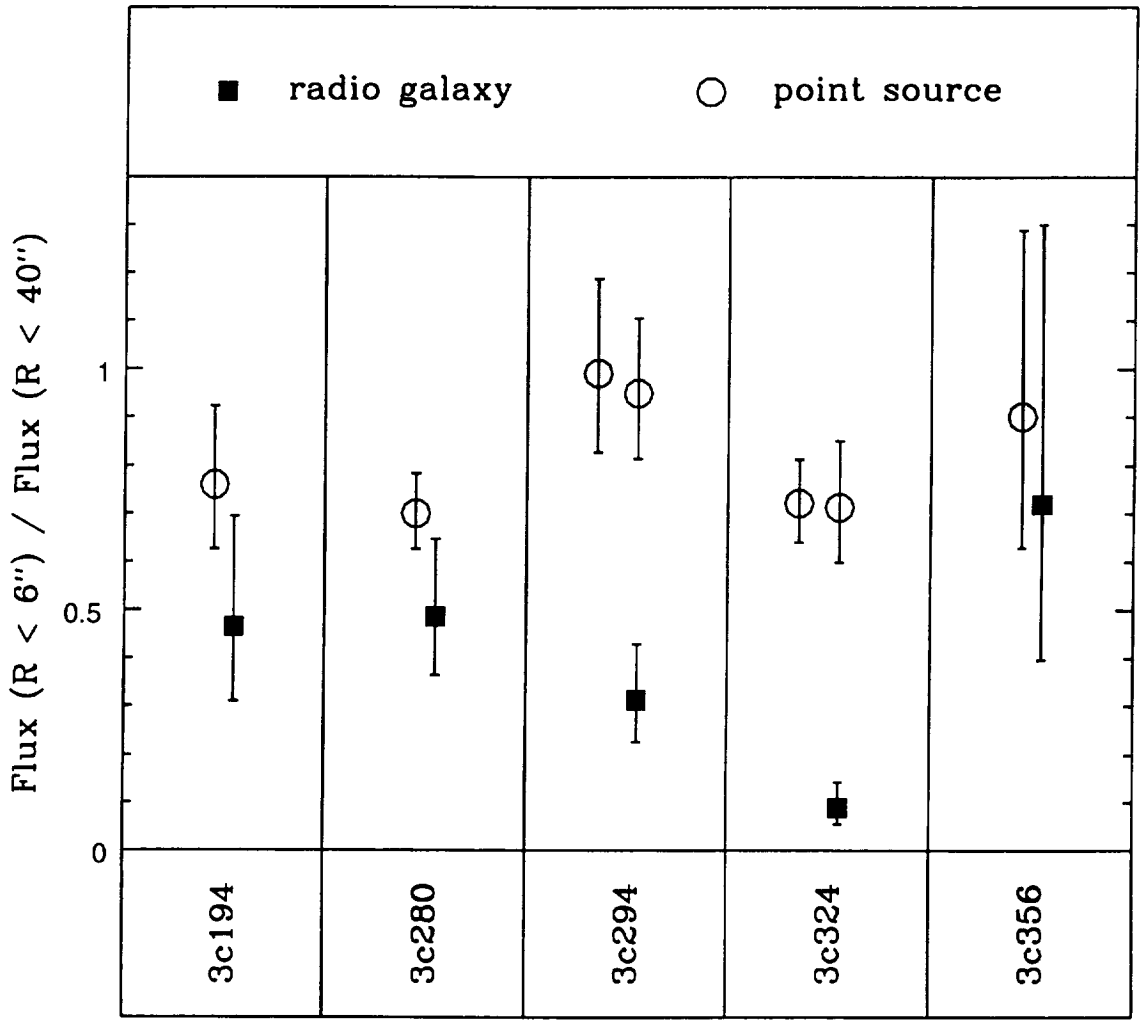

Fig. 3.— Ratio of fluxes measured from small (6″) and large (40″) apertures in the HRI images. This ratio provides a rough measure of the spatial extent of the X–ray emission – point–like sources should have approximately 75% of their energy encircled within a 6″ radius, while for extended sources the fraction would be smaller. One or more measurements of actual point sources are shown for each radio galaxy field, along with the radio galaxy itself. 3C 194, 3C 280 and 3C 356 appear to be only marginally extended in this test, while 3C 294 and 3C 324 are both clearly resolved.

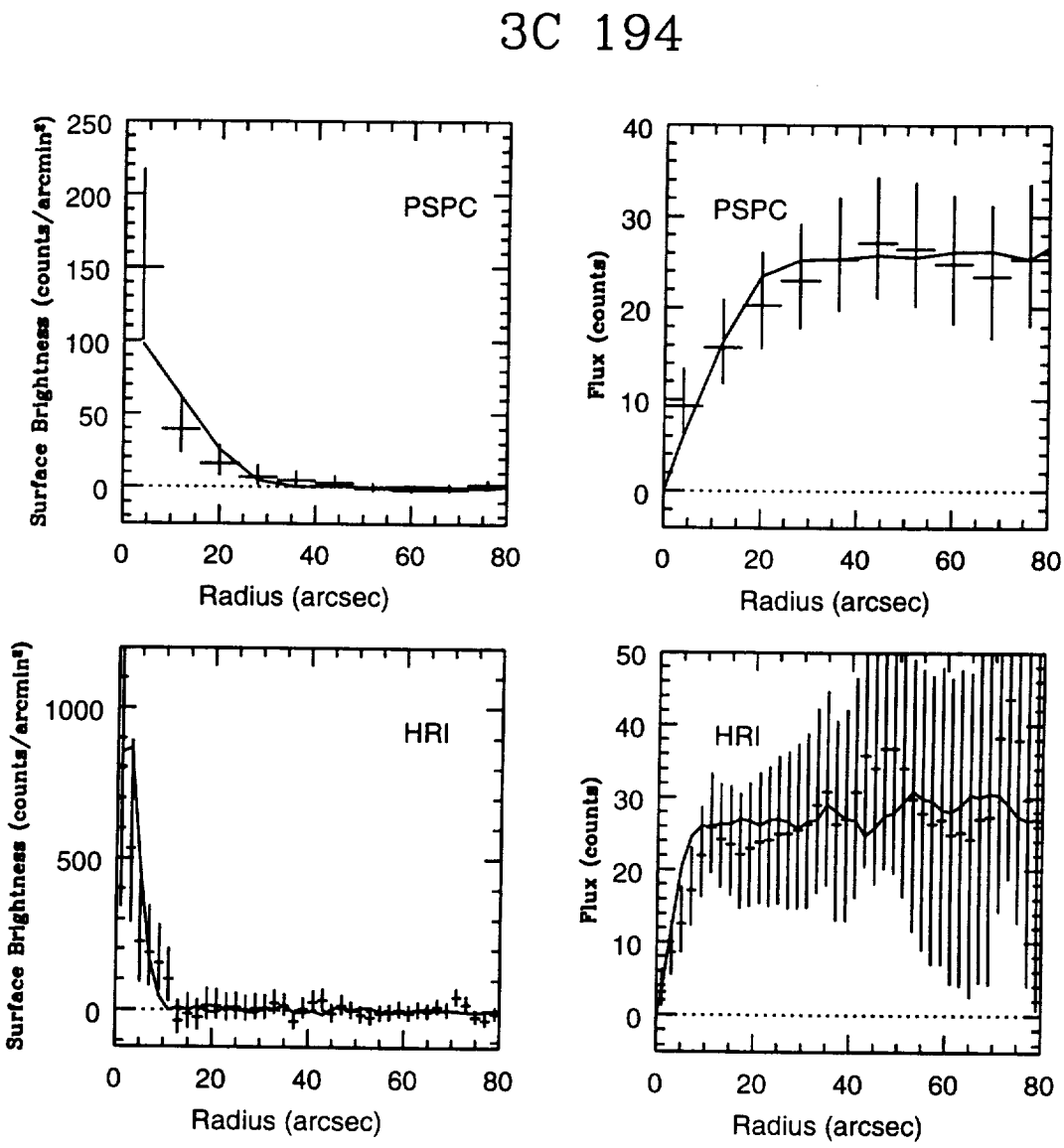

Fig. 4.— Radial profiles of the X–ray emission from 3C 194 in the PSPC (top) and HRI (bottom). The differential surface brightness profile is shown at left, while the integrated curve of growth for the flux is shown at right. The radio galaxy data are shown as a crosses whose vertical extent indicates the 1σ Poisson measurement uncertainties. The solid line shows the profile for a serendipitous point source in the same data set which has been multiplicatively rescaled to have the same integrated flux as does radio galaxy. The X–ray emission from 3C 194 is very compact in both the PSPC and HRI images. There may be extended flux in excess of the point source model at radii of 5–10″(see also figure 3) but its formal significance is low.

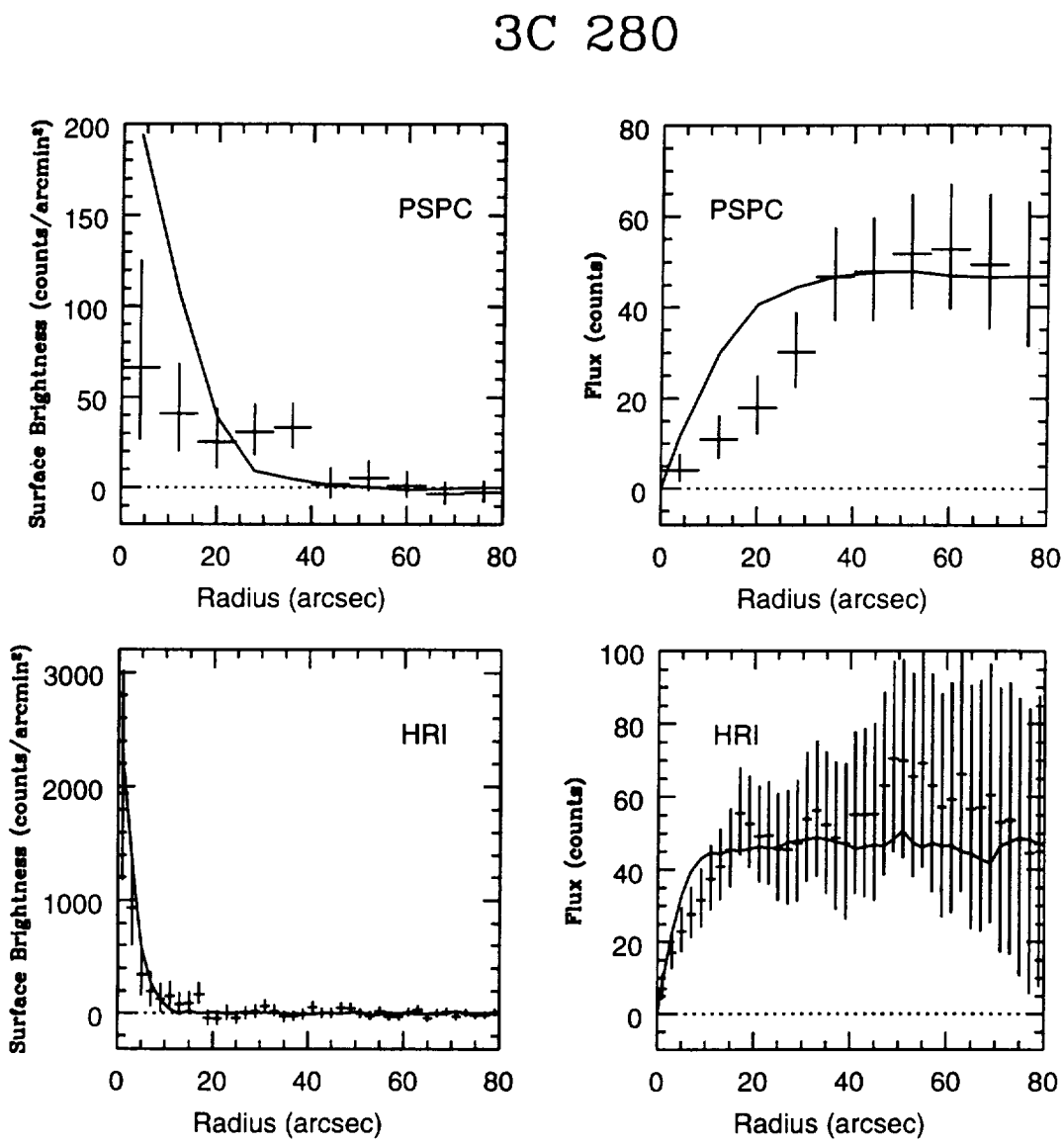

Fig. 5.— Same as figure 4 but for 3C 280. Here the PSPC image appears to be spatially extended, while the HRI data shows a strong compact, probably point source component. It is unclear whether there is also an extended component to the HRI emission – see text for discussion.

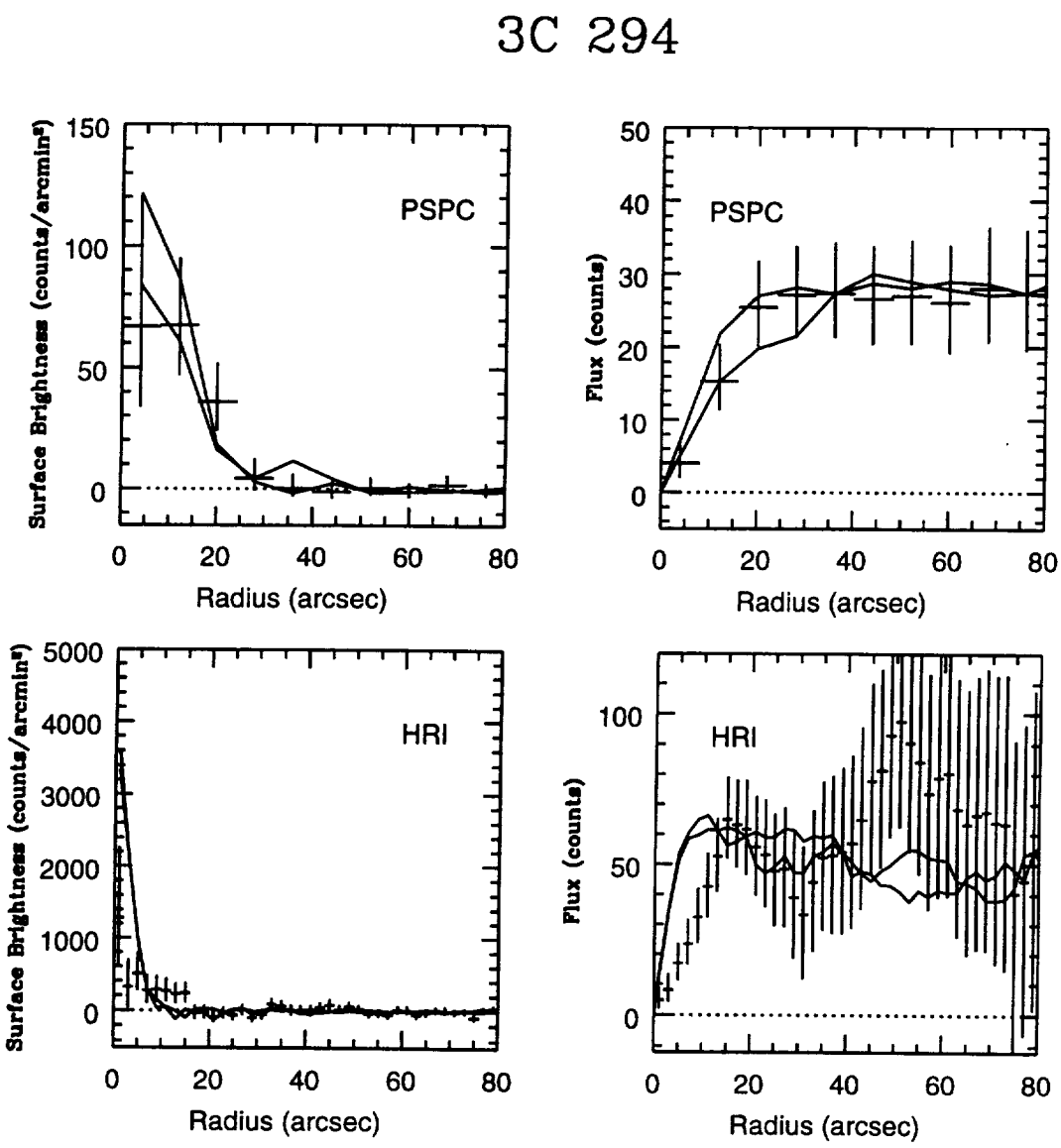

Fig. 6.— Same as figure 4 but for 3C 294. The X–ray emission is probably unresolved by the PSPC, but is clearly extended in the HRI. Note how the profiles of the point sources have much higher central peak surface brightness values than does that from 3C 294 itself, despite the fact that both have been normalized to the same integrated flux.

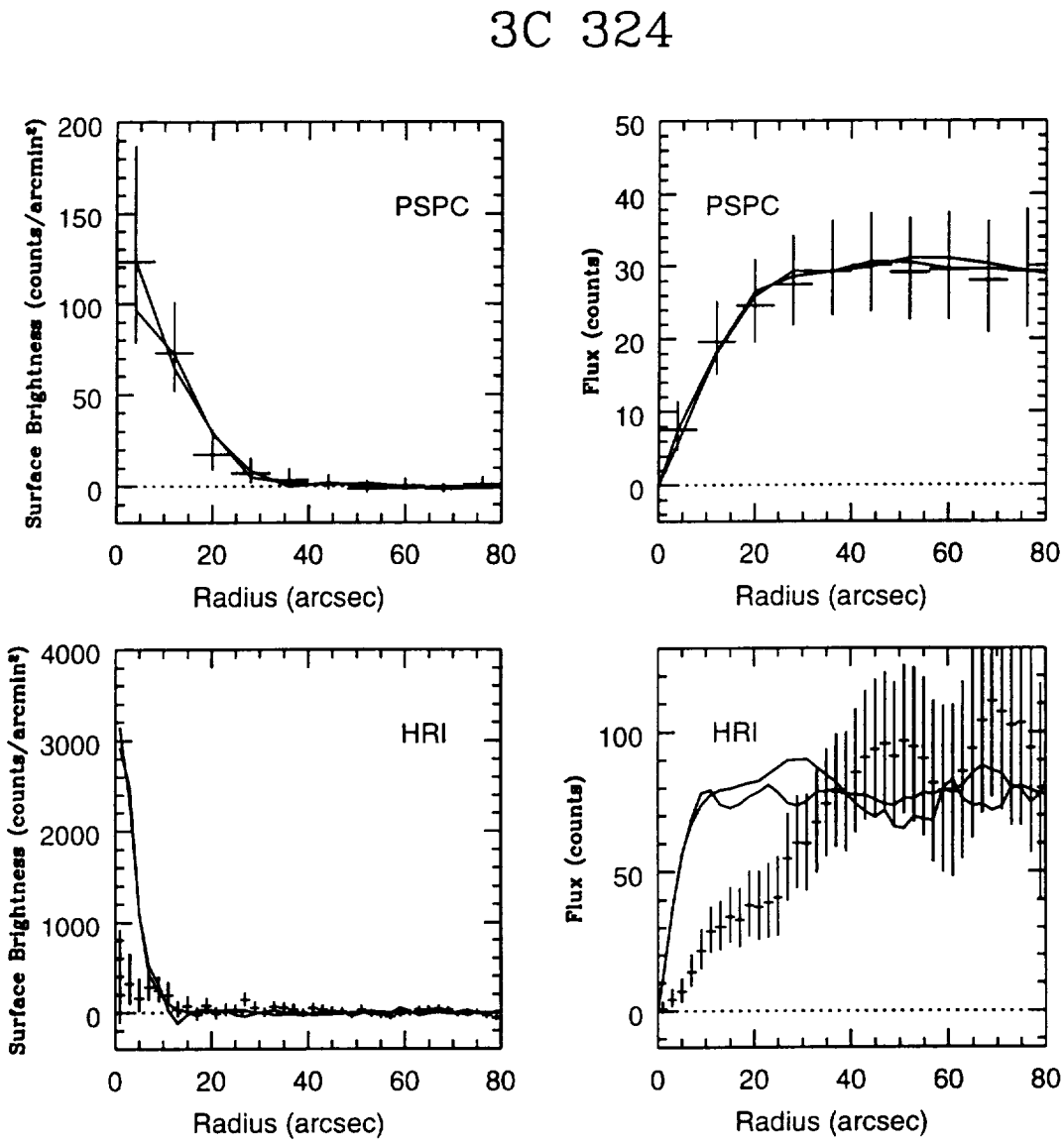

Fig. 7.— Same as figure 4 but for 3C 324. The radio galaxy is not readily distinguishable from the point sources at PSPC resolution, but in the HRI it is clearly resolved, exhibiting a broader profile with lower peak surface brightness than do the point sources. X–ray emission from the radio galaxy environment is detected out to a radius of at least 40″, or > 300 kpc.

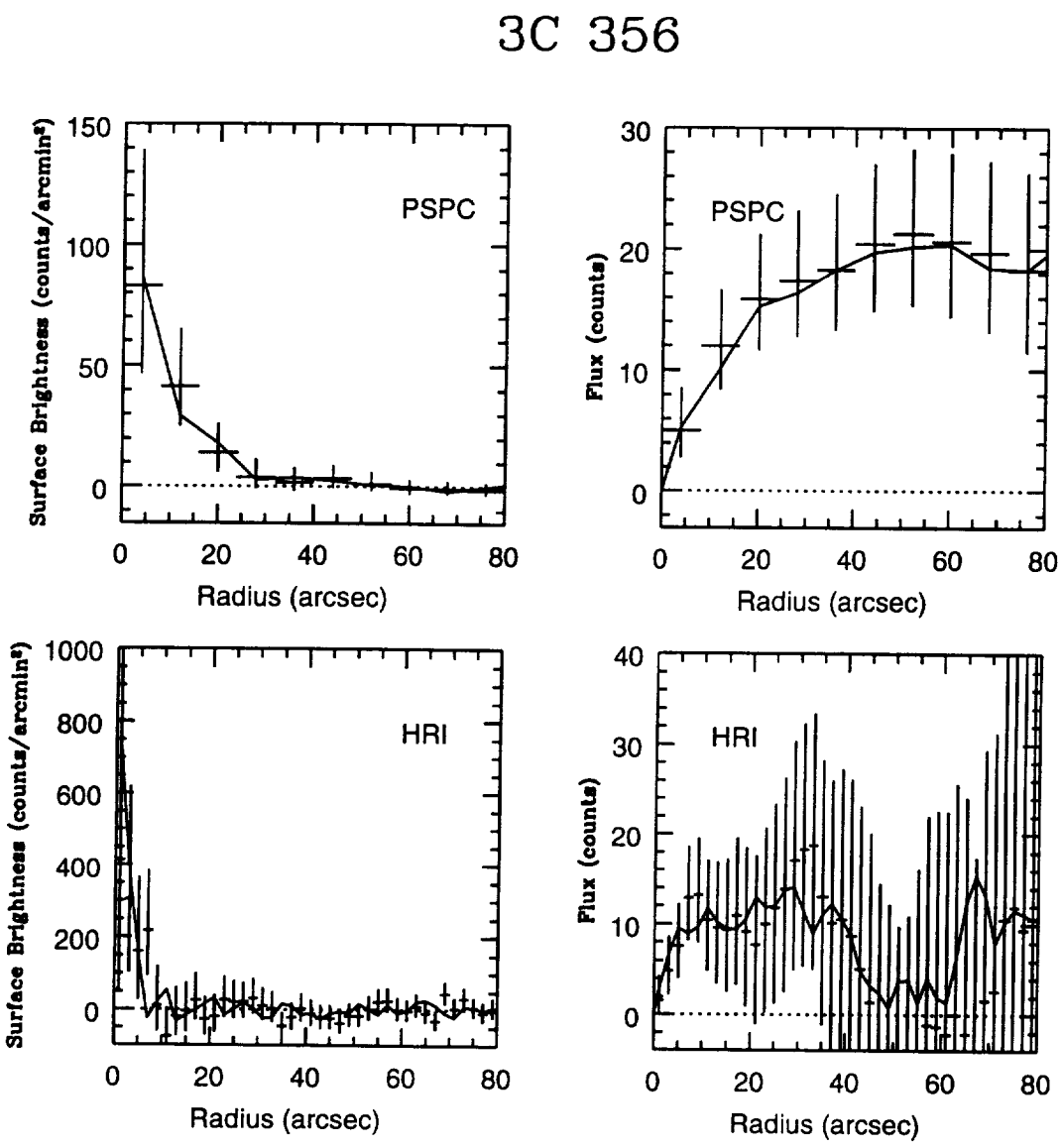

Fig. 8.— Same as figure 4 but for 3C 356. Here the HRI data has rather low signal-to-noise – the encircled flux is only marginally positive (S/N < 1) in our standard 40″measurement aperture, although it appears to be significantly detected at smaller radii. The source, if detected, appears to be fairly compact.

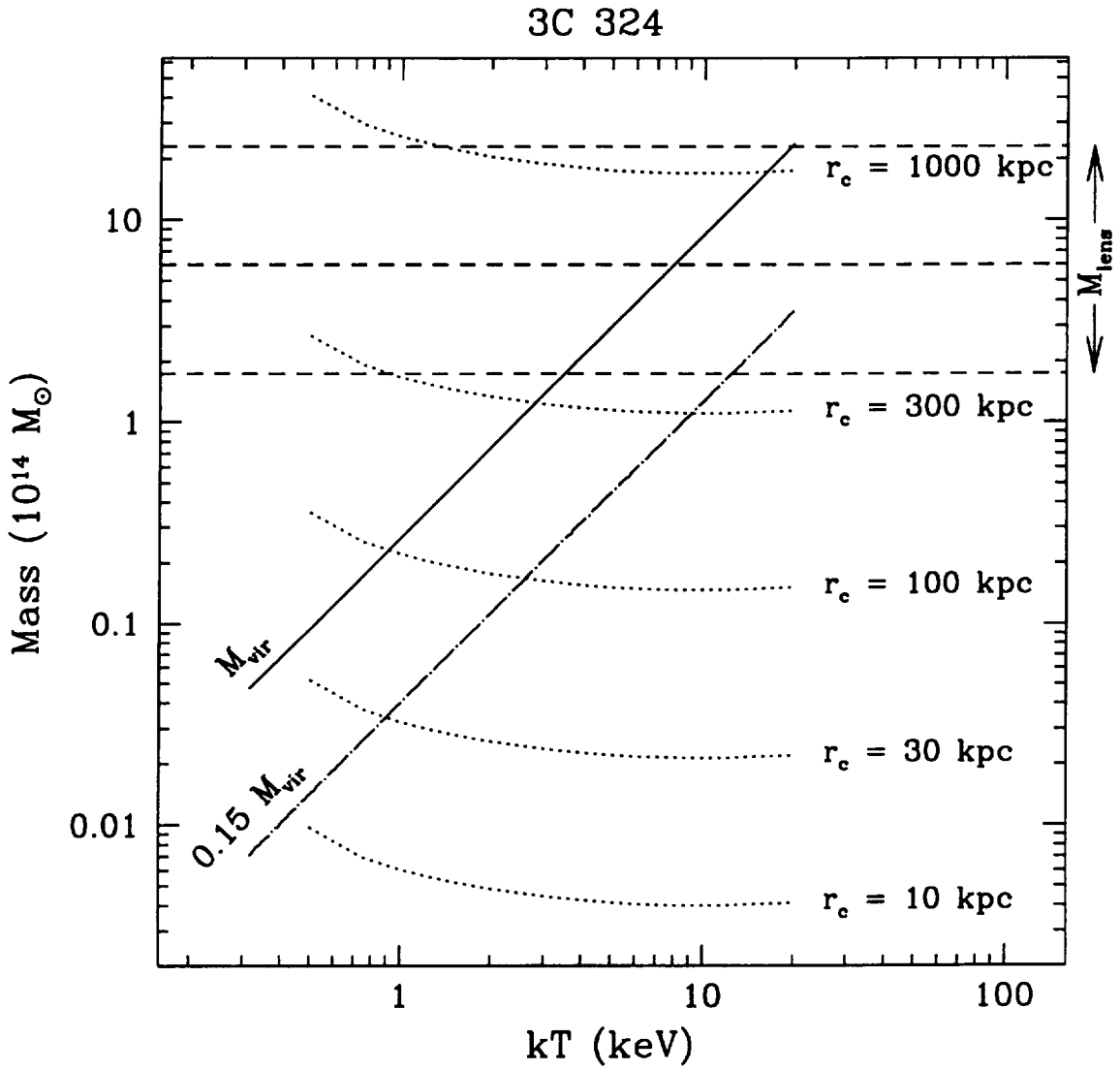

Fig. 9.— Computed virial and gas masses for the 3C 324 cluster as a function of temperature. The solid line shows the predicted $M_{\rm vir}$ for a cluster with virial temperature kT at $z = 1.206$. The dot–dash line below this indicates the corresponding gas mass if $M_{\rm gas}/M_{\rm vir} = 0.15$, a typical value for nearby rich clusters. The dotted lines show gas masses derived from the observed X–ray luminosity assuming a $\beta = 2/3$ gas density profile (eq. 1) for various values of the X–ray core radius. Denser X–ray gas (smaller r_c) requires less mass to produce the same luminosity. The dashed horizontal lines show the limiting range of masses (within a 1.0 Mpc radius) derived from the weak lensing measurement of Smail & Dickinson (1995). All computations assume an $H_0 = 50$ km s^{-1} Mpc^{-1}, $\Omega_M = 1$ cosmology.

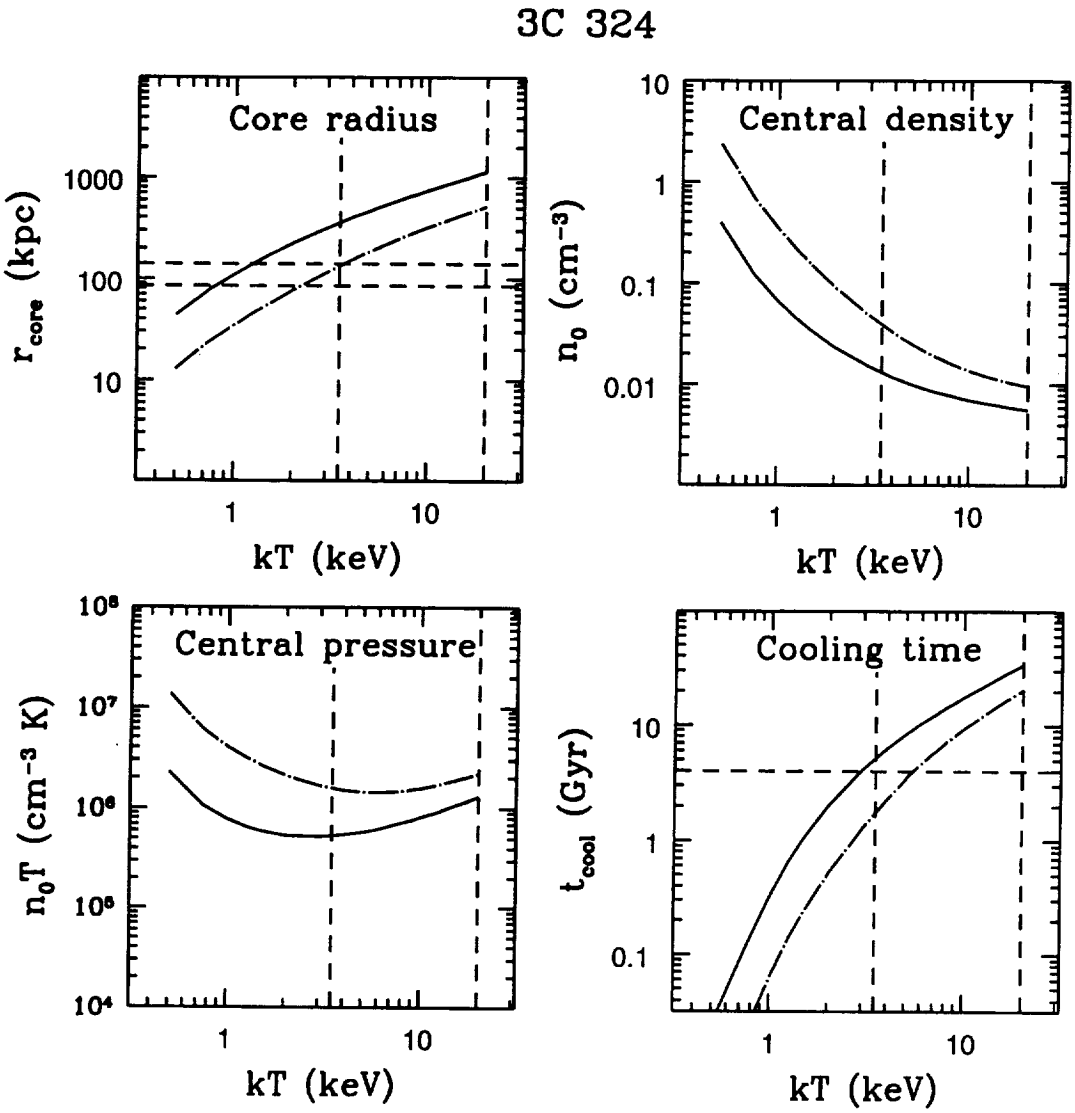

Fig. 10.— Derived quantities for 3C 324 X–ray gas, assuming the condition $M_{\rm gas} = M_{\rm vir}$ (solid lines) or $M_{\rm gas} = 0.15 M_{\rm vir}$ (dot–dashed lines). In each panel the vertical dashed lines indicate the virial temperature range (3.5–20 keV) implied by the lensing mass measurement. Upper left: X–ray core radius. The horizontal lines show the lower and upper limits (85–140 kpc) for the core radius derived from the ROSAT images. Upper right: central gas (total particle number) density. Lower left: central pressure. Lower right: radiative cooling time. The age of the universe at $z = 1.206$ is marked in this panel as a horizontal dashed line. $H_0 = 50$, $\Omega_M = 1$ has been assumed throughout.

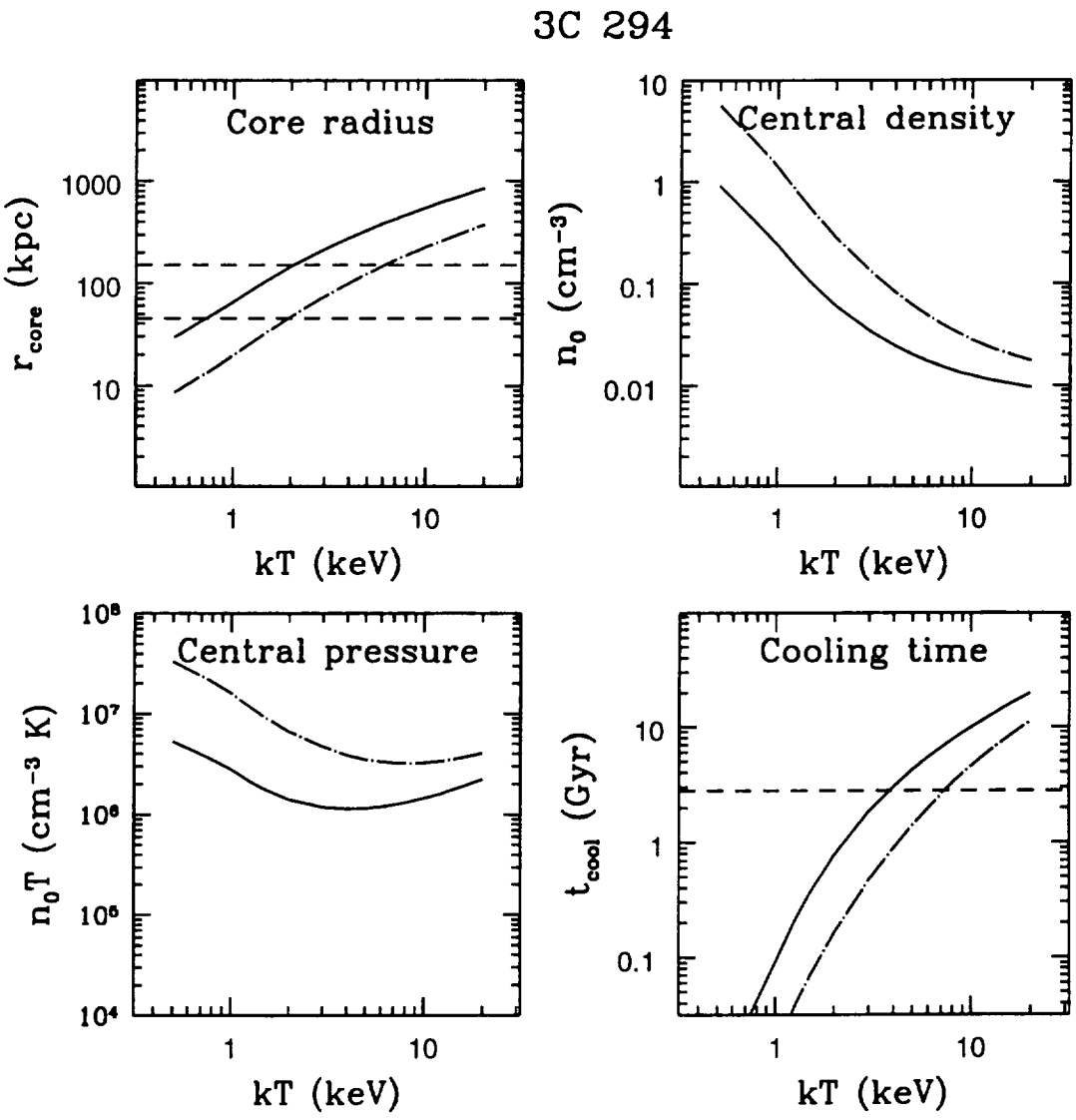

Fig. 11.— Derived quantities for 3C 294 X–ray gas – the panels and meaning of the different line types is the same as for figure 10, except that for 3C 294 there is no constraint on the virial temperature from gravitational lensing.

Table 1. ROSAT Observations

			PSPC				HRI		
Object	z	$\log(N_H)$[a] (cm^{-2})	Exposure (sec)	Measured[b] Counts	Flux[c]/10^{-14} (erg s^{-1} cm^{-2})	L_X[d]/10^{44} (erg s^{-1})	Exposure (sec)	Predicted Counts	Measured[b] Counts
3c194	1.184	20.69	7853	$25.3^{+6.7}_{-5.6}$	$5.1^{+1.3}_{-1.1}$	$4.0^{+1.1}_{-0.9}$	31762	$41.2^{+10.9}_{-9.1}$	$27.0^{+15.0}_{-13.9}$
3c280	0.998	20.06	47610	$46.8^{+10.8}_{-9.8}$	$1.4^{+0.3}_{-0.3}$	$0.7^{+0.2}_{-0.2}$	62985	$28.9^{+6.7}_{-6.1}$	$47.2^{+21.7}_{-20.7}$
3c294	1.786	20.08	22456	$27.3^{+7.0}_{-5.9}$	$1.7^{+0.4}_{-0.4}$	$3.2^{+0.8}_{-0.7}$	94135	$55.9^{+14.3}_{-12.1}$	$54.1^{+28.0}_{-27.0}$
3c324	1.206	20.63	15427	$29.3^{+7.1}_{-6.0}$	$2.9^{+0.7}_{-0.6}$	$2.4^{+0.6}_{-0.5}$	72117	$56.0^{+13.6}_{-11.5}$	$78.0^{+21.7}_{-20.7}$
3c356	1.079	20.44	18563	$18.3^{+6.1}_{-5.0}$	$1.4^{+0.5}_{-0.4}$	$0.9^{+0.3}_{-0.3}$	36379	$15.3^{+5.1}_{-4.2}$	$10.5^{+16.7}_{-15.6}$

[a]Galactic foreground HI column density from Stark et al. (1992).

[b]Counts measured within a 40″ radius aperture.

[c]Flux in 0.4–2.4 keV band within 40″ radius aperture, assuming redshifted Raymond–Smith thermal spectrum with $kT = 4$ keV and abundance 0.3 × cosmic, corrected for galactic foreground absorption.

[d]Luminosity in rest-frame 1–5 keV band, computed for $H_0 = 50$ km s^{-1} Mpc^{-1} and $q_0 = 0.5$ assuming the same spectral model.

SPACE TELESCOPE SCIENCE INSTITUTE

3700 San Martin Drive
Baltimore, MD 21218
(410) 338-4700
FAX (410) 338-4767

December 8, 1999

Mr. Bradley Poston
Grants Officer - 210.G
National Aeronautics and Space Administration
Goddard Space Flight Center
Greenbelt, MD. 20771

Reference: NAG5-3209
STScI WBS# J0467
PI: Dr. Mark Dickinson
Final Reports

Dear Mr. Poston,

I am pleased to submit the Final Reports for the above referenced grant entitled, "*The Most Distant X-Ray clusters*"under the direction of Dr. Mark Dickinson. Please find enclosed the Final Technical, Final Financial, Final Property and Patent & Inventions Reports.

Should you have questions or require additional information, please contact me at 410.338.4364 or *larisad@stsci.edu.*

Sincerely,

Larisa Dolhancryk
Sponsored Programs Administrator I

Enclosure

cc: CASI, Acquisitions Dept.
ONR, Closeout Team